

Implementing Embedded Speed Control for Brushless DC Motors

Part 1

Yashvant Jani
Renesas Technology America, Inc.
450 Holger way, San Jose CA 95134
408-383-7716

yashvant.jani@renesas.com

Abstract

Brushless Direct Current (BLDC) motors, also known as permanent magnet motors, are used today in many applications. A new generation of microcontrollers and advanced electronics has overcome the challenge of implementing required control functions, making BLDC motors more practical for a wide range of uses.

This two-part seminar covers BLDC motor control fundamentals and implementation techniques. Part 1 discusses 120-degree trapezoidal control with and without sensors, while Part 2 covers 180-degree sine wave modulation and V/f open-loop and closed-loop control with sensors. Topics discussed include interrupt handling for pulse width modulation (PWM) generation and sensor processing with performance measurement for CPU bandwidth usage. Implementation of a speed profile (speed vs. time) and its interface with the interrupt handler are also described.

Part 1: Introduction

We begin Part 1 of this seminar with the basics of BLDC motors, including their construction and operation. Fundamental equations for force and torque generation are presented, along with the basic control electronics necessary for proper deployment. We discuss 120-degree modulation and a six-step method for operating the motor. Then we see how the modulation can be implemented using Hall sensors and back-EMF signals. Implementation examples make use of a microcontroller unit (MCU), which leads to a discussion of the necessary features of on-chip timers and interrupt handling within the MCU.

We next review the source code for six-step operation prior to discussing trapezoidal speed control, which in BLDC motors is typically implemented using the six-step method. This type of closed-loop control allows designers to control motor speed with proper accuracy, and examples show how the MCU can be used in speed control.

BLDC fundamentals

A BLDC motor has two main components: a rotor made up of permanent magnets and a stator with a winding connected to the control electronics. The brushes and commutation ring that are essential parts of a universal motor have been eliminated from the BLDC motor design. Instead, control electronics are used to generate a proper sequence for commutation. Because of its design, the BLDC motor is also known by other names: permanent magnet synchronous motor (PMSM), brushless permanent magnet motors, or permanent magnet AC (PMAC) motor. Sometimes it is simply called a PM motor.

The BLDC motor is based on a fundamental principle of magnetism, which tells us that similar poles repel each other, while opposite poles attract. As Figure 1a illustrates, when a current is passed through two coils, it generates a magnetic field with a polarity that creates torque on the central magnet—in this case, the rotor. When a current is passed in the direction shown, the central rotor rotates clockwise. When the rotor reaches a certain position, the direction of the current is changed so that the torque continues further in the same direction. When necessary, the current direction is changed again to continue generation of the torque. However, instead of two coils, actual BLDC motors typically use six coils positioned 60 degrees apart, as indicated by Figure 1b. Then, two coils at a time can be energized to create a torque sufficient to move the rotor to a desired position. When this position is reached, other coils are energized to continue producing the torque.

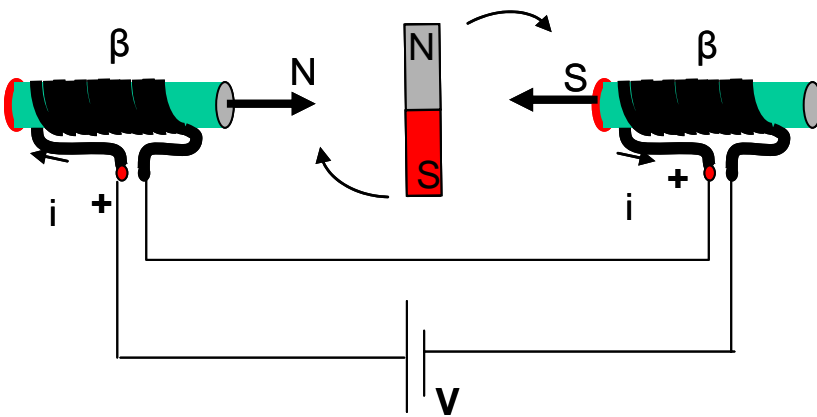


Figure 1a. Magnetic field due to current in stator coils creates torque on the rotor.

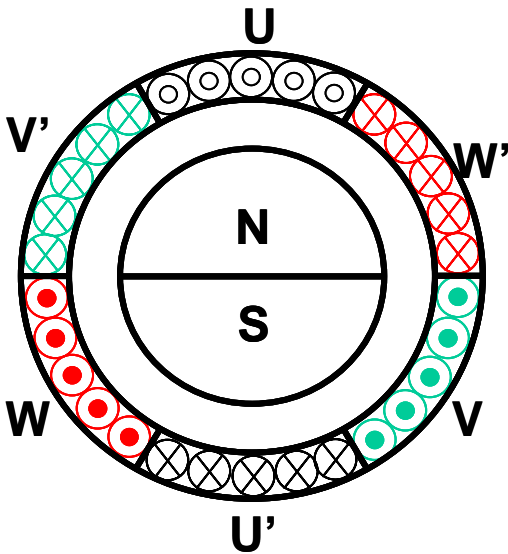


Figure 1b. Single pole pair 3-phase motor has six stator coils.

The total amount of torque created on the rotor is calculated using the Lorentz force formula in scalar form:

$$\text{Torque } T = r * F = r * (i * L * \beta * \text{Sin } \theta).$$

Here, r is the moment arm of the rotor, i is the current passing through stator coils, L is the length of coil, β is the magnetic field of the rotor, and θ is the angle between the current direction and the magnetic field of the rotor. The larger the current, the larger the torque in the motor because the magnetic field and winding length remain the same once the motor has been constructed. Designers have only one quantity to change during motor operation: the current.

In vector form, this formula is $T = r \times F$, where all three quantities are given in vector form with magnitude and direction. This formula is important because it allows designers to create an algorithm based on vector formulation when they want to control torque and the flux in the motor.

A BLDC motor offers many advantages over other types of motors. Its speed is not impeded by the stress limitations of brushes. Because it has no brushes to create sparks, the motor can be used in hazardous environments. It is efficient, reliable, and generally low maintenance. The torque-speed relationship is

linear. Also, a high torque-to-volume ratio means that a BLDC motor requires less copper (metal) than do other motor types.

BLDC motors do have some drawbacks, though. Rotor position information is required for proper operation, so either Hall sensors or a back-EMF signal with intelligence must be used to obtain this information. In general, the motor requires external power electronics, whereas an AC induction motor achieves constant-speed operation when started from and driven by an AC power supply. The BLDC motor is a 3-phase device. As such, it requires an inverter and, thus, a power switch. Its rotor requires magnetic (rare-earth) metal, so it may cost more. Finally, incorrect control of a BLDC motor, especially at high temperatures, can damage its permanent magnet, so careful design of the control electronics is essential.

Despite these drawbacks, use of BLDC motors abounds in the industry. Several examples are illustrated in the following figures. Figure 2 shows the GE Electronically Commutated Motor (ECM), which has 12 poles (six pole-pairs) and comes in various horsepower ratings. Its electronics are mounted at the end of the motor in a case that is the same diameter as the motor itself. The GE ECM is a 3-phase motor that accepts a single-phase AC supply. Its stator has 18 coils and the rotor has surface-mounted magnets. Notice that the rotor is located inside the motor and stator is on the outside.

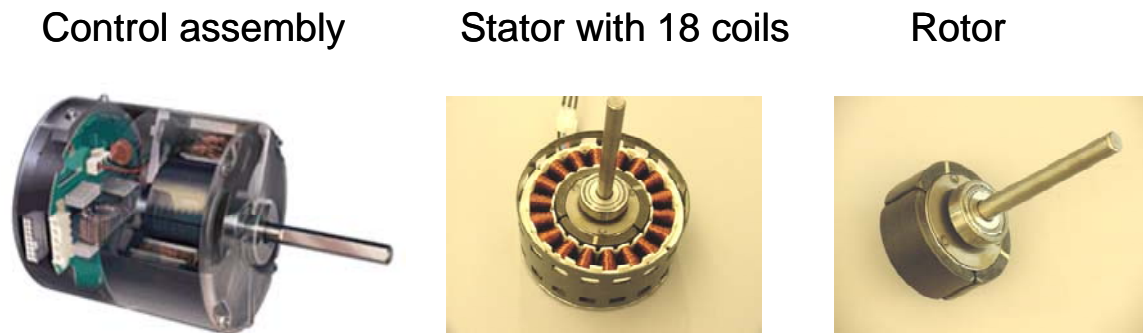


Figure 2. Electronically Commutated Motor (ECM) with control assembly.

In contrast, the pancake motor shown in Figure 3 positions the rotor on the outside and the stator inside. The rotor has several surface-mounted magnets, and the stator has many coils. The small, low horsepower motor shown in Figure 4 (slide 6, right figures) has external stators and internal rotors. All of these BLDC motors offer high torque and low volume, giving them an edge over universal or AC induction motors for applications in small spaces.

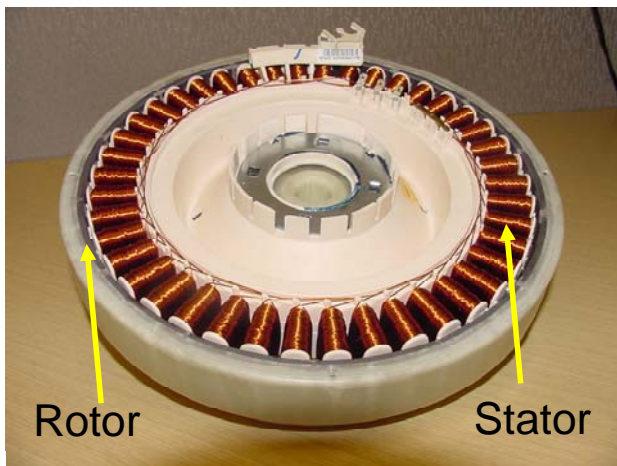


Figure 3 Pancake motor assembly shows stator and rotor.

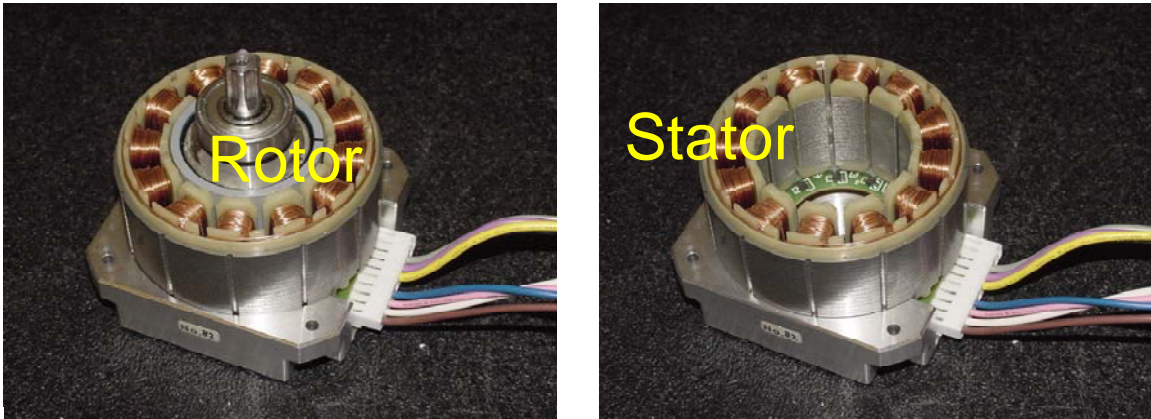


Figure 4. Small Brushless DC motor for appliance applications.

BLDC motor control

In Figure 5a we see that the stators in 3-phase BLDC motors are connected in a Y or a star formation. All three phases are connected in the center, which is called the neutral or $\frac{1}{2} V_{dc}$ point. For this type of connection, the sum of the currents in all three phases is zero. Note that only two currents have to be measured; the third can be derived easily.

$$I_{sa} + I_{sb} + I_{sc} = 0$$

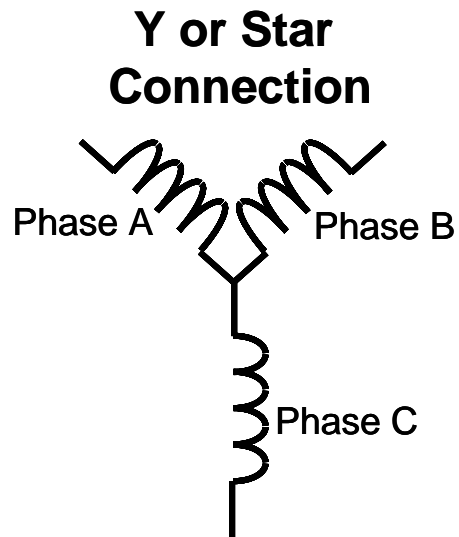


Figure 5a. Star or Y-winding for the stator has sum of currents equal to zero.

The stator-per-phase circuit shown in Figure 5b has one inductive element and one resistive element. Its torque is proportional to the current as long as the magnetic field does not change.

Stator per phase circuit

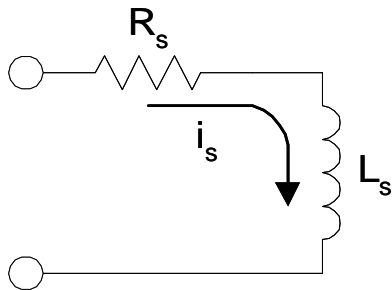


Figure 5b. Stator equivalent circuit.

In this case, torque is $T = k \Phi i_s$, where k is constant, Φ is the magnetic field, and i_s is the stator current. If we combine k and Φ , we can write simply $T = K * i_s$, where K is known as the torque constant. The amount of current passing through the stator coils is based on the voltage applied and the back-EMF voltage generated. As the motor starts rotating, it generates more back-EMF voltage, which reduces the current and results in less torque. The diagram in Figure 5c (slide 7) shows that as the current increases, speed increases up to a certain point and then becomes constant. Torque increases up to a certain point and then decreases. This behavior is typical in a BLDC motor. Flux is pre-established by the magnetic field of the rotor. Therefore, torque is controlled simply by controlling the current in the stator. The commutation sequence ensures that the rotor rotates in synchronization with the stator excitation.

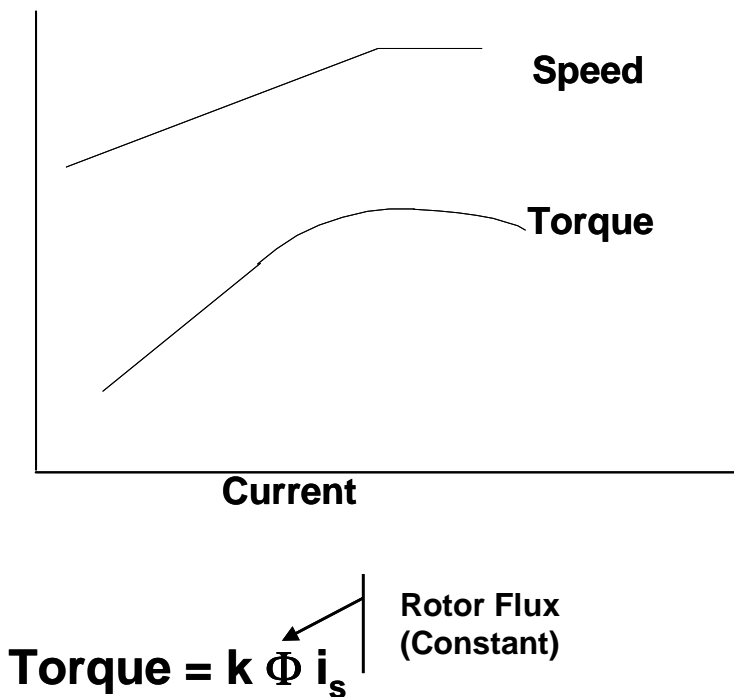


Figure 5c. Torque and speed increases as current increases in the stator coils.

Typical hardware used to control a BLDC motor are the converter and inverter is shown in Figure 6a. Six power-MOSFET or insulated-gate bipolar transistor (IGBT) switches are used in the inverter. When AC to DC conversion is not required, a DC supply can be connected directly to the inverter board. A typical BLDC motor drive configuration is shown in Figure 6b (slide 8). Notice that the power switches are labeled

S1 – S6 in this figure. They have other common names, which can be used according to the author’s preference. Thus,

- S1 = $U_p = U^+ = A^+$
- S2 = $U_n = U^- = A^-$
- S3 = $V_p = V^+ = B^+$
- S4 = $V_n = V^- = B^-$
- S5 = $W_p = W^+ = C^+$
- S6 = $W_n = W^- = C^-$

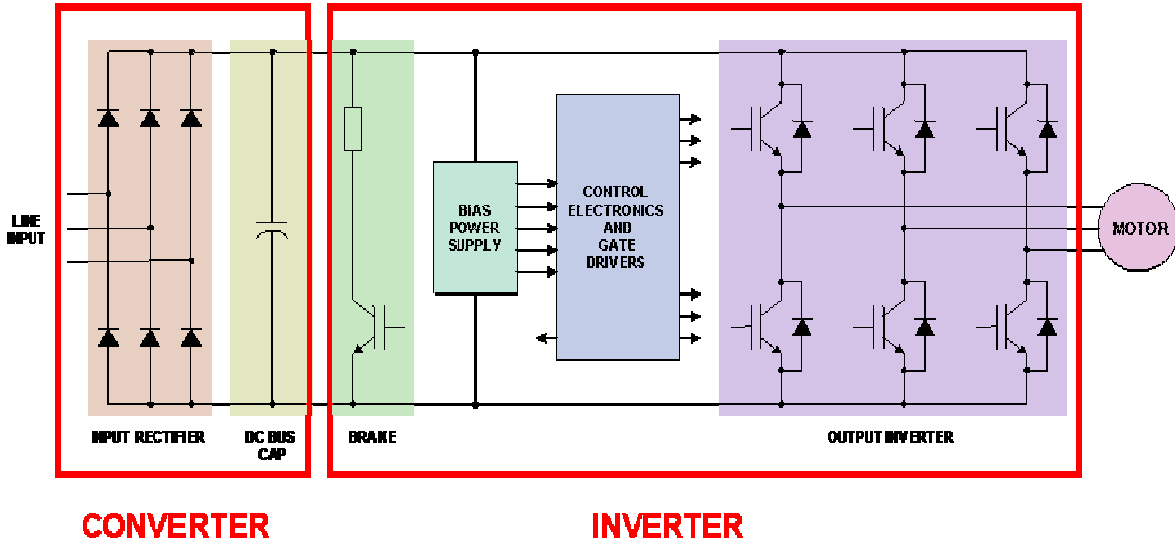


Figure 6a. Typical hardware layout with converter and inverter modules.

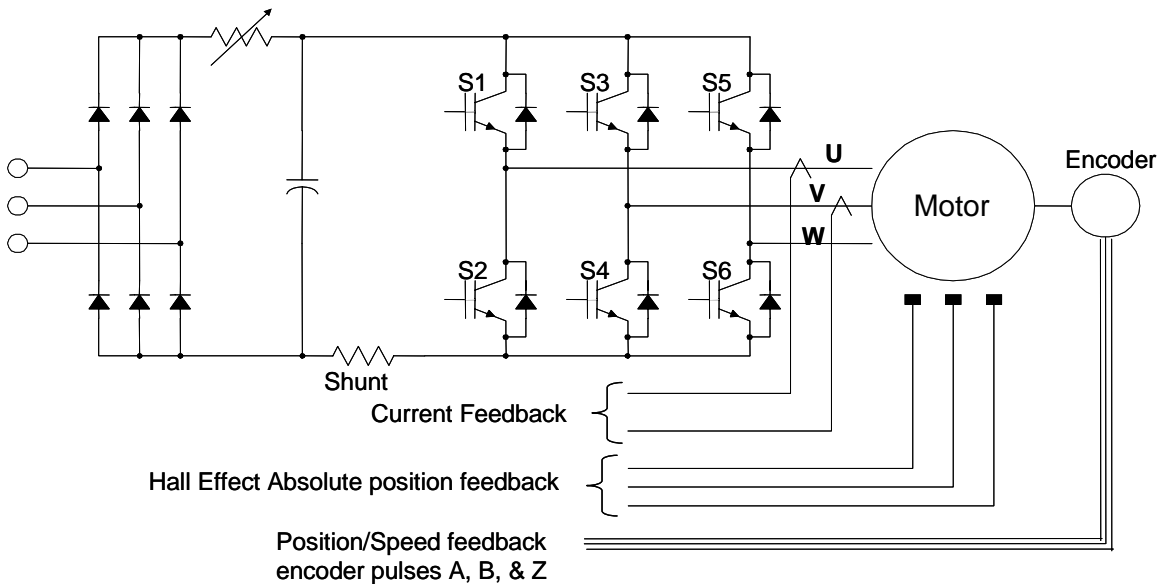


Figure 6b. Typical representation with six switch configuration.

A BLDC motor also has sensors. For example, Hall sensors and an encoder may be used to provide information about the position of the rotor. These sensors are not connected with the commutation and control portion of the inverter and MCU. However, because the MCU must process signals from these sensors, they must interface with the MCU. Hall sensors and the encoder are connected to the rotor, and rotation is necessary to create Hall signals.

Back-EMF signals are created from the high side of the phase voltage using a resistor ladder. Current can be measured using DC current transducers (DCCT) or AC current transducers (ACCT) with phase wires passing through the coils. Additionally, certain techniques allow single-phase currents to be measured using a shunt resistor. The back-EMF and DCCT/ACCT or shunt resistor are connected to the stator.

In motor terminology, control based on Hall sensors and an encoder is known as control with sensors, while control without these elements is known as sensorless control.

120-degree modulation and commutation sequence

As Figure 1b illustrates, a BLDC motor has six coils with phase settings generally denoted as U_p , U_n , V_p , V_n , W_p , and W_n . (Alternatively, we can use U_+ , U_- , V_+ , V_- , W_+ , and W_- to indicate these settings.) Three Hall sensors are located 120 degrees apart around the stator. Depending on which magnetic field passes over each sensor, the output may be high or low. When the north pole passes over a sensor, its output is high or state 1. When the south pole passes over a sensor, its output is low or state 0. Hall sensors thus provide information about polarity and position.

A six-step commutation sequence is used to steer the current and produce torque. The sequence starts with the initial position of the rotor aligned properly at 0 degrees. Power at the coils U_+ and V_- is turned on. This excitation creates a magnetic field so that the rotor turns in the intended direction—towards the 60-degree position. When this position is reached, V_- is turned off and W_- is turned on. Because U_+ is still on, the U_+ and W_- coils are excited, and torque continues in the same direction.

When the rotor reaches the 120-degree position, U_+ is switched off and V_+ is switched on. W_- is still on and so the V_+ and W_- excitation continues to produce torque in the same direction. At the 180-degree position, W_- is turned off and U_- is turned on, while V_+ is kept on. At 240 degrees, V_+ is turned off and W_+ is turned on, with U_- kept on. At 300 degrees, U_- is turned off and V_- is turned on, and W_+ is kept on. Finally, when the rotor completes a 360-degree rotation, W_+ is turned off and U_+ is turned on, with V_- kept on. Thus, we are back to the original state or step 1.

These six steps, depicted in Table I, form the commutation sequence that produces correct rotation in one direction. For rotation in the reverse direction, the steps are executed in reverse order: 1, 6, 5, 4, 3, 2 and back to 1.

Table I. Six steps for 120-degree modulation.

Step #	Phase U_p	Phase V_p	Phase W_p	Phase U_n	Phase V_n	Phase W_n
1	U_p				V_n	
2	U_p					W_n
3		V_p				W_n
4		V_p		U_n		
5			W_p	U_n		
6			W_p		V_n	

In our description, 'step' is synonymous with 'state'. Figure 7 shows the complete six-step sequence with angles given in units of radians. Figure 7 also shows the current flow as it enters from one coil and exits a second coil. This current flow corresponds exactly to the six steps of turning the switches on and off. Since each positive phase (U_+ , V_+ , and W_+) is energized for 120-degree rotation, and each negative phase (U_- , V_- , and W_-) is also energized for 120-degree rotation, this type of modulation is called 120-degree modulation. At each of six steps, one power-MOSFET or IGBT is switched on or off, hence the term 120-degree six-step commutation. Figure 8 illustrates these principles in a 120-degree drive system.

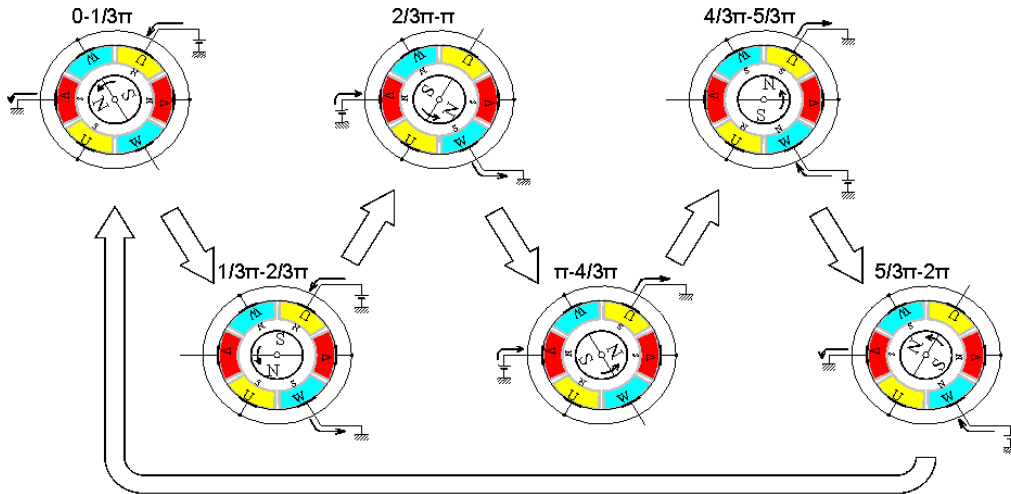


Figure 7. Six step modulation for Brushless DC motor.

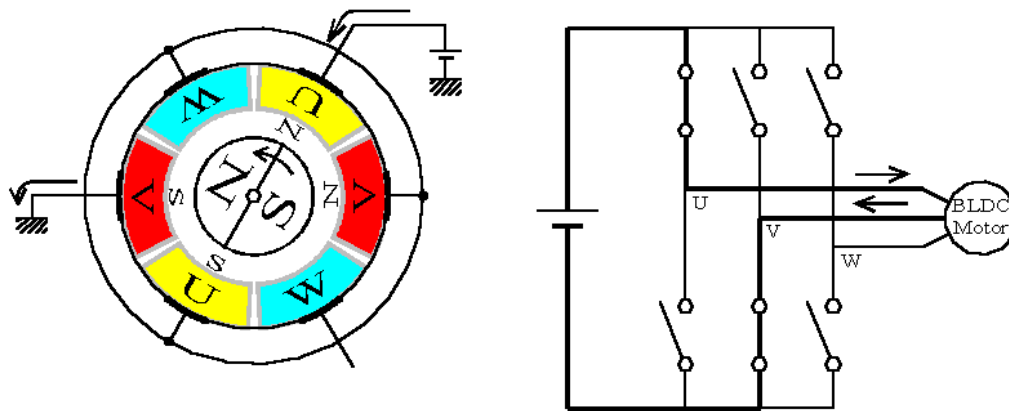
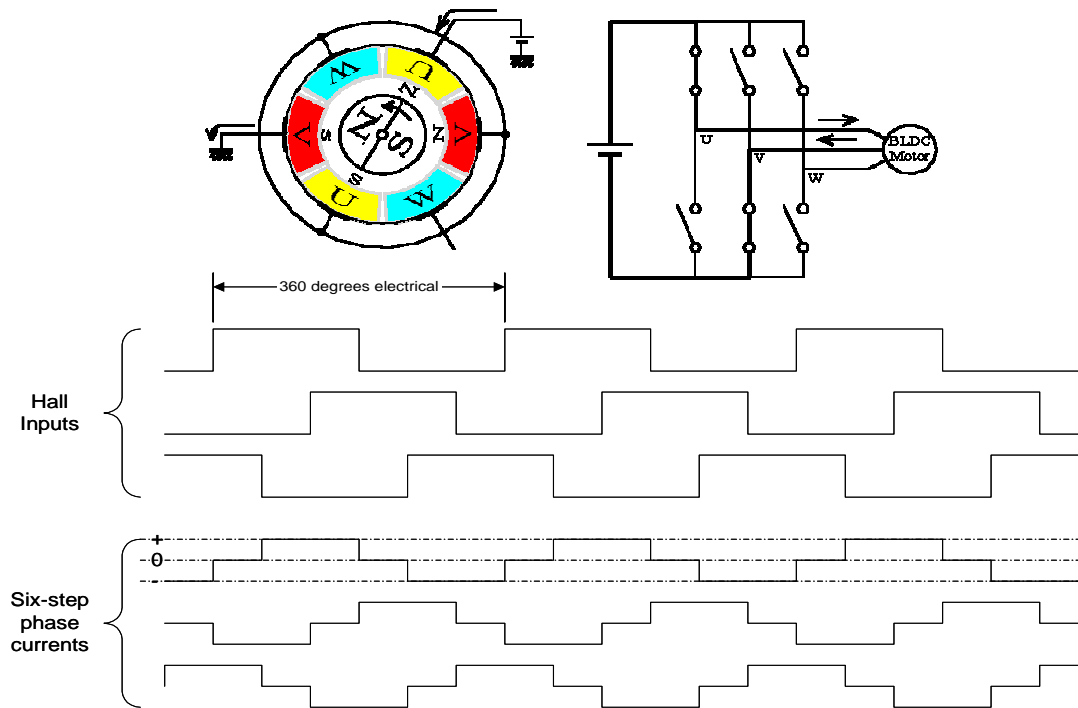


Figure 8. Six steps modulation with switch configuration.

Control electronics—in particular the MCU—play an important role in this operation. Hall-effect signals are fed into MCU as external interrupts. With every interrupt signal, the MCU performs a state change; in other words, it turns off one switch device and turns on another one. The MCU performs its task by executing interrupt-based code and changing the state of the output pin. The MCU has three interrupt input pins, one for each Hall sensor, and six output pins, one for each switch driver.

The operation of a motor with 120-degree six-step commutation, along with the behavior of the phase currents, is shown in Figure 9.



Typical 6-step commutation (only 2 phase conducting at any time)
 This is typical of inverters without 3-phase peripheral and PMSM with Hall Effects.

Figure 9. Six step commutation with phase currents behavior.

Implementation example

Let's consider the example of Hall sensor signal processing. At every interrupt, the MCU has to execute a code that properly changes the output state. This interrupt-based code must interpret the Hall signals correctly and then change power-switch states, first turning off one switch and then turning on the next.

Since Hall sensors provide polarity, we can easily determine which Hall sensor interrupt has been received by reading all three polarity levels. A Hall sensor set-up in which rising Hall signals occur at every 120-degree position is shown in Figure 10 (slide 17). Notice that the rising U Hall signal is at 0 degrees, the rising V Hall signal is at 120 degrees, and the rising W Hall signal is at 240 degrees. Because Hall sensors have a south pole located 180 degrees from the north pole, a falling signal will occur at the 180-degree offset of each rising signal, thus creating six signals over the complete rotation.

On receiving the first interrupt—the rising edge of Hall A—the MCU firmware reads the three interrupt input pins as 1, 0, 1 and sets the output pins to state 1, with U_p and V_n on. On receiving the second interrupt—the falling edge of Hall C—the MCU firmware reads the input pins as 1, 0, 0; compares this reading to the previous state (1, 0, 1); and sets state 2. On receiving the third interrupt—the rising edge of Hall B—the MCU reads the input pins as 1, 1, 0; compares the reading to 1, 0, 0 and sets state 3. The next three interrupts are processed in a similar manner to complete the cycle.

In this example, we need to know which sensor is A, which is B, and which is C. Motor manufacturers generally provide this information. Nevertheless, it's instructive and helpful to lay out the board, connect the motor, power up the MCU only (not the entire motor), and view the signals from the Hall sensors, which get their power from the MCU board. Now we can examine the sequence of Hall signals easily, turning the motor by hand for one complete rotation. The signals can also be viewed on a scope as the motor is rotated to determine whether or not they are 120-degree Hall signals.

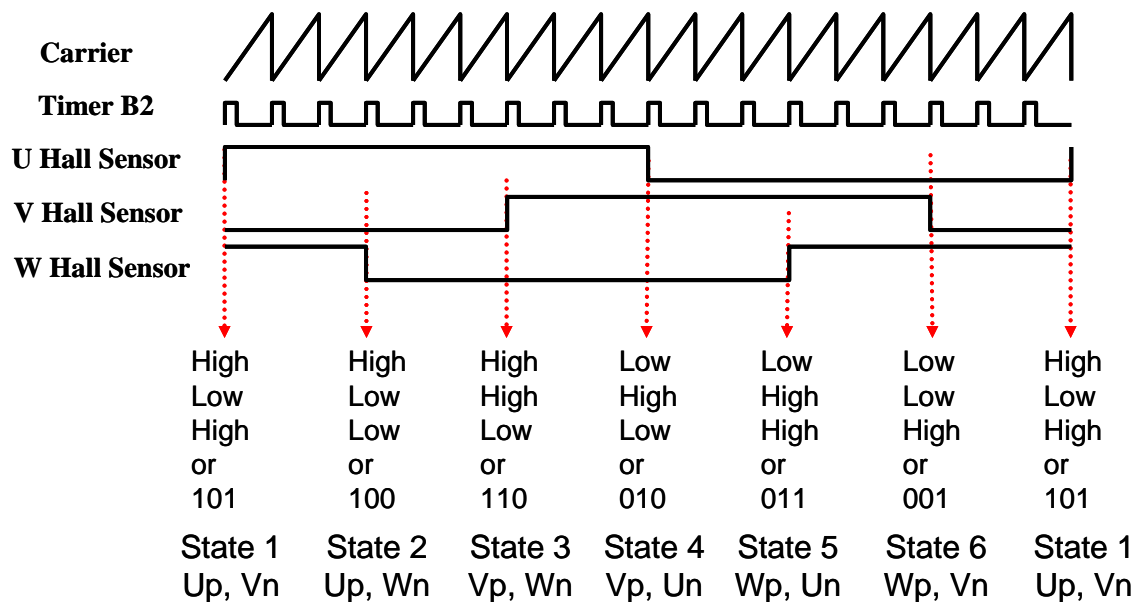


Figure 10. Six step changes for 120 deg input Hall sensors.

If we observe 60-degree Hall signals, which means that the rising edge occurs every 60 degrees rather than every 120 degrees, then the sequence of inputs changes as shown in Figure 11 (slide 19). On the first interrupt, the firmware reads 1, 0, 0 instead of 1, 0, 1. The sensor changes to a state-1 configuration in which Up and Vn are still on. It does not change to the state-2 configuration used in the 120-degree example. On the next interrupt, the sensor reads the input pins as 1, 1, 0 and then the firmware makes the change to state 2. The cycle continues according to the sequence of Hall signals. Notice that the firmware is changed slightly and the sequence of Hall input signals is different. For proper sensor implementation, designers must know how the Hall sensors are mounted and how the firmware should be written.

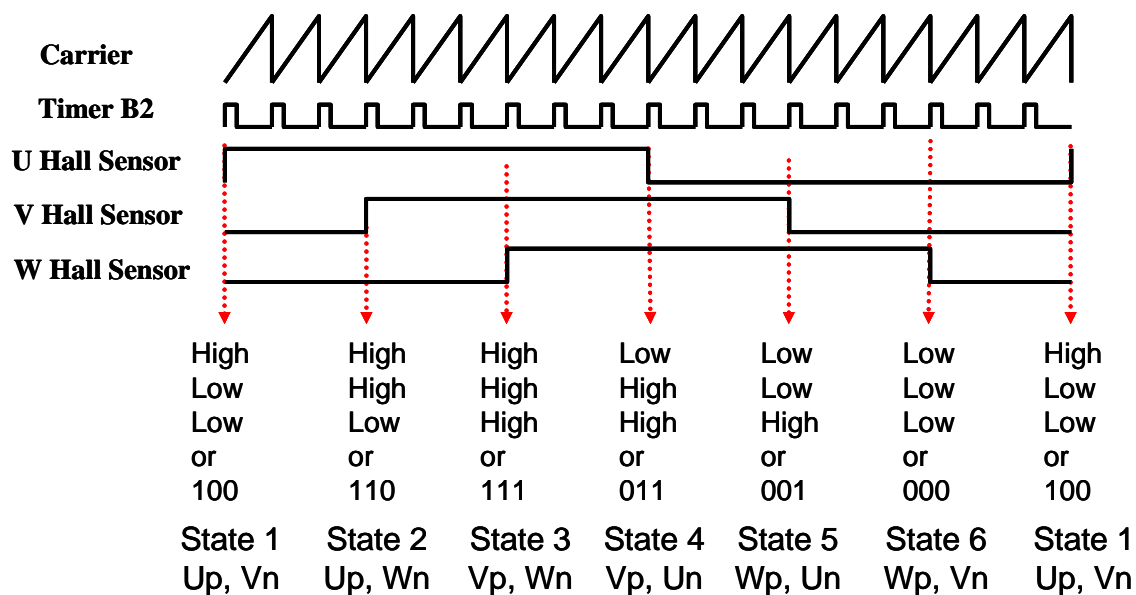


Figure 11. Six step changes for Hall sensors mounted 60 deg rising signals.

Table II further compares two Hall-sensor configurations. Again, the best way to implement the firmware is to perform some initial tests to determine what is necessary for rotation in one direction and what is

necessary for rotation in the reverse direction. Once this information is available, the firmware can be implemented easily, including the correct rotational sequence.

It's important to note that these examples are based on a one pole-pair motor. A motor that has more pole pairs will have a larger sequence on the signals in one mechanical rotation. For example, a Bodine motor has two pole pairs, and so instead of six interrupts, it has 12 interrupts per mechanical rotation. Thus, when tests are performed to obtain the sequence of Hall signals, the motor must be rotated slowly, smoothly, and continuously—otherwise, the sequence observed may be incorrect.

Table II. Comparison of two Hall-sensor configurations.

Interrupt	Rising Hall signal	Sequence	Rising Hall signal	Sequence
1	A	1, 0, 1	A	1, 0, 0
2		1, 0, 0	B	1, 1, 0
3	B	1, 1, 0	C	1, 1, 1
4		0, 1, 0		0, 1, 1
5	C	0, 1, 1		0, 0, 1
6		0, 0, 1		0, 0, 0

The C programming code for a commutation sequence for the Renesas R8C MCU is shown in Figure 12. The case statements are translated into a compact code size by the compiler. Individual phase voltages and voltages between U-V, V-W and W-U are shown in Figure 13.

```

Switch (stg_p) /* Implement Appropriate State for Control */
case 0:
    p1_1 = 0;          /* VP Off */
    p1_2 = 0;          /* WP Off */
    p3_0 = 0;          /* UN Off */
    p3_2 = 0;          /* WN Off */
    p3_1 = 1;          /* VN On */
    p1_0 = 1;          /* UP On */
    break;
case 1:
    p1_1 = 0;          /* VP Off */
    p1_2 = 0;          /* WP Off */
    p3_0 = 0;          /* UN Off */
    p3_1 = 0;          /* VN Off */
    p3_2 = 1;          /* WN On */
    p1_0 = 1;          /* UP On */
    break;
case 2:
    p1_0 = 0;          /* UP Off */
    p1_2 = 0;          /* WP Off */
    p3_0 = 0;          /* UN Off */
    p3_1 = 0;          /* VN Off */
    p3_2 = 1;          /* WN On */
    p1_1 = 1;          /* VP On */
    break;
case 3:
    p1_0 = 0;          /* UP Off */
    p1_2 = 0;          /* WP Off */
    p3_1 = 0;          /* VN Off */
    p3_2 = 0;          /* WN Off */
    p3_0 = 1;          /* UN On */
    p1_1 = 1;          /* VP On */
    break;
case 4:
    p1_0 = 0;          /* UP Off */
    p1_1 = 0;          /* VP Off */
    p3_1 = 0;          /* VN Off */
    p3_2 = 0;          /* WN Off */
    p3_0 = 1;          /* UN On */
    p1_2 = 1;          /* WP On */
    break;
case 5:
    p1_0 = 0;          /* UP Off */
    p1_1 = 0;          /* VP Off */
    p3_0 = 0;          /* UN Off */
    p3_2 = 0;          /* WN Off */
    p3_1 = 1;          /* VN On */
    p1_2 = 1;          /* WP On */
}

```

Figure 12. R8C code in C language for 6 step changes for BLDC motor.

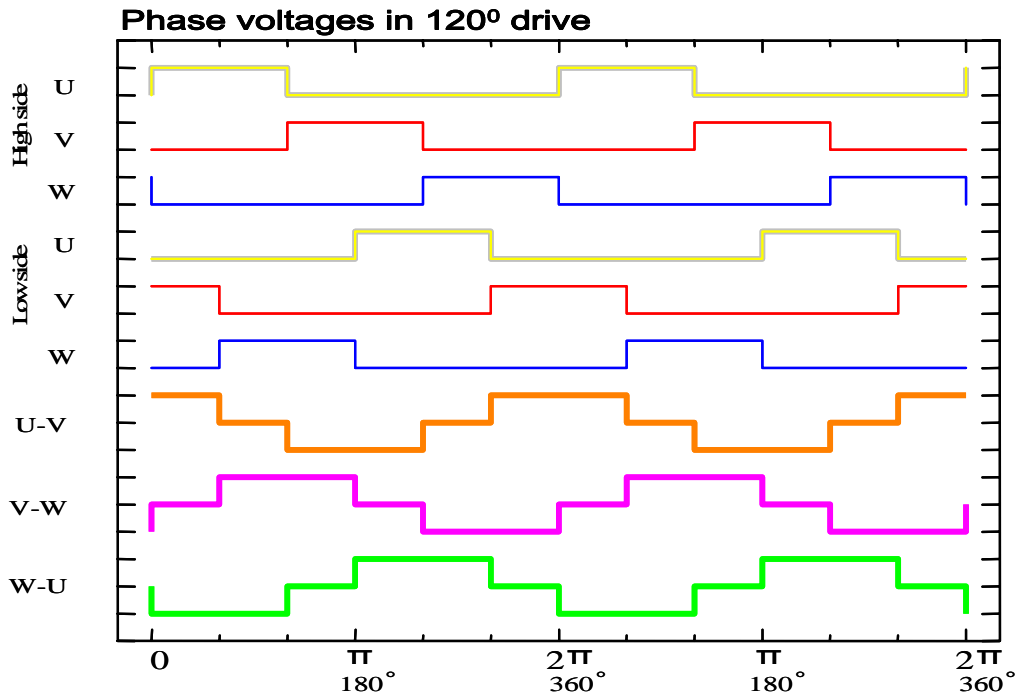


Figure 13. Phase voltages for six step trapezoidal control.

Trapezoidal control with Hall sensors

To understand trapezoidal control in a BLDC motor, let's first consider full-speed operation. When a full voltage is turned on every 120 degrees of rotation, and when proper commutation is performed according to the Hall-signal inputs, the motor rotates at its full operational speed. The MCU receives interrupt inputs and properly executes outputs according to the sequence desired.

The full speed at which the motor operates is determined by certain characteristics. The applied voltage and back-EMF are balanced so that the torque necessary to maintain operational speed is achieved. Figure 14 shows a current profile—that is, the shape of the currents—at full speed with input Hall signals and six-step currents. Notice that the shape of the phase currents is trapezoidal. As we have seen before, torque in BLDC motors is proportional to the current passing through the coils. Therefore, to reduce the speed, we must reduce the current. Torque is maintained at the necessary level by changing the current to maintain the desired speed.

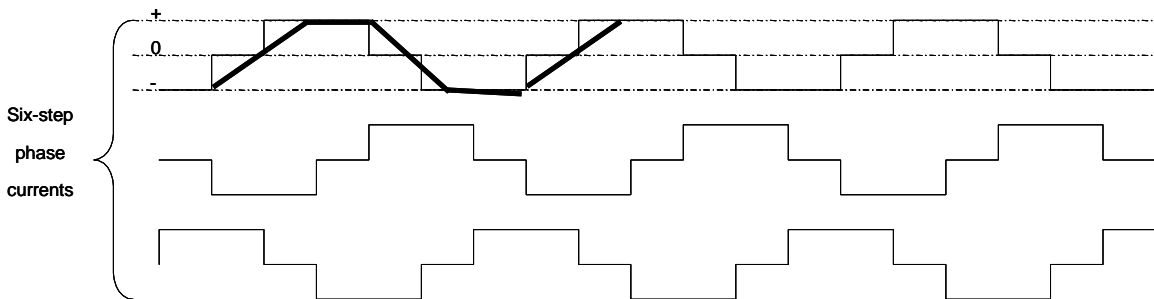


Figure 14. Current at full speed operation is trapezoidal and hence the name “Trapezoidal” control.

To reduce the current in coils, voltage is modulated using the pulse width modulation (PWM) method illustrated in Figure 15. During a state, the voltage is turned on and off at a suitable frequency, known as the carrier frequency, in a manner that applies less current to each coil. As a result, less torque is created on

the rotor and speed is reduced. A PWM timer is used to modulate the output state of the pin and thus the voltage applied to the phase. This modulation is typically performed at a carrier frequency higher than the state-change frequency. Even when the voltage is modulated, the current profile remains trapezoidal—thus the name, trapezoidal control.

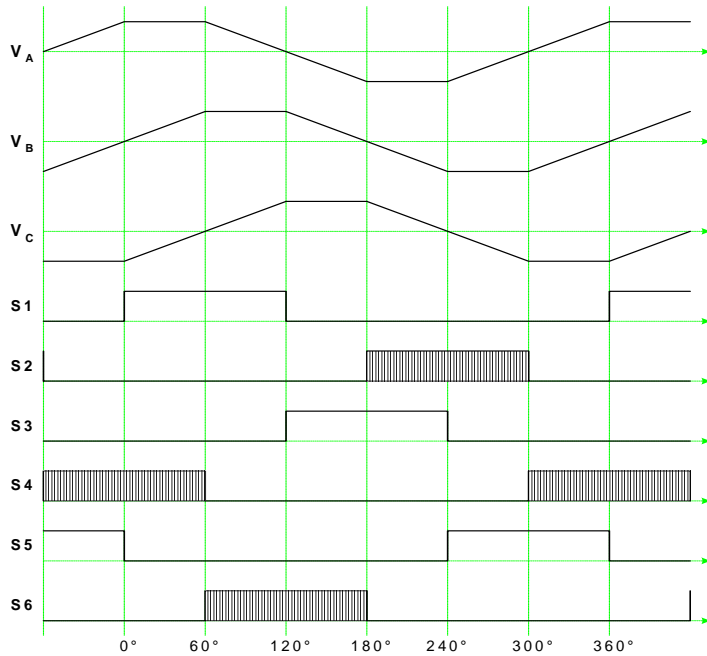
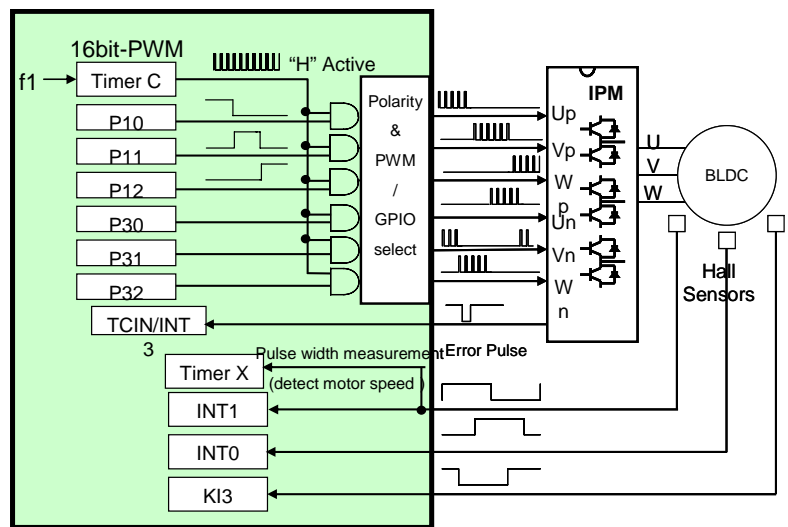


Figure 15 Trapezoidal currents with modulation in lower switches.

The PWM method requires us to know carrier frequency and duty cycle. We can select an arbitrary frequency for the carrier signal we will modulate. But how do we know what duty cycle is needed to maintain the desired speed? Hall sensors come to rescue again, as speed can be measured using the Hall-signal interrupts. The angle between two consecutive Hall signals is 60 degrees by construction, and these signals are mapped onto the interrupt pins by the MCU.



Using an MCU timer peripheral, the time between two consecutive Hall signals can be measured and speed can be computed: It's 60 degrees divided by the time measured between two Hall signals. To determine average speed, we can measure the time between six or more Hall signal interrupts, whatever is suitable in terms of time to control the speed. Now it becomes easy to adjust the duty cycle. If the measured speed is high, the duty cycle is reduced. If the measured speed is low, the duty cycle is increased.

Figure 16. R8C based BLDC control.

The MCU resources required for this activity include six output pins, three input pins, one internal timer to measure the time between two consecutive Hall signals. We also need one PWM timer that can modulate

each output pin, or a timer that can generate six outputs properly with modulation, as well as one interrupt for emergency shut-down. These resources are depicted in Figure 16, in which an R8C is the MCU.

Timing example

Now let's consider an example of how timing is used in speed control. Assume that we have a BLDC motor that has two pole pairs and a maximum operational speed of 3600 RPM. The MCU is running on a 20-MHz CPU clock, and that clock is also used for the timers and counters.

Our calculations will be based on the following formulas:

$$\begin{aligned} \text{Speed (Hz)} &= \text{Speed (RPM)} / 60 = \text{mechanical Hz} \\ \text{Mechanical Hz} &= 60 \end{aligned}$$

$$\begin{aligned} \text{Electrical Hz} &= \text{\#pole pairs} * \text{mechanical Hz} \\ \text{Electrical Hz} &= 120 \end{aligned}$$

$$\begin{aligned} \text{Electrical time period or period} &= 1/\text{electrical Hz}; \\ \text{Period} &= 1/120 = 8.3333 \text{ ms} = 8333.3 \mu\text{s} \end{aligned}$$

$$\begin{aligned} \text{Time } t_H \text{ between two Hall signals} &= \text{electrical Hz} / 6; \\ t_H &= 8333.3 / 6 = 1388.9 \mu\text{s} \end{aligned}$$

$$\begin{aligned} \text{Counts between two Hall signals} &= \text{Count Frequency in MHz} * \text{time between two Hall signals} \\ \text{Counts} &= 20 * 1388.9 = 27,778 \text{ counts in our example.} \end{aligned}$$

When we fix the counting frequency at 20 MHz and the pole-pair equal to 2, the formula can be simplified to give

$$\text{Counts} = 100,000,000 / \text{RPM}$$

This is a very simple formula.

Next we can prepare a table that gives RPM and corresponding counts. It's important to check at what RPM the size of the 16-bit counter will become an issue. In the example above, at 1200 RPM the count value is 83,333, which causes the counter to overflow. In fact, for a count less than 65,535, the minimum RPM is 1535. Therefore, a 16-bit counter driven by a 20-MHz clock is usable only as long as the motor speed stays above 1535 RPM. See Table III.

Table III. Counts for various reference speeds.

Number	Speed in RPM	Counts
1	1200	83,333 *
2	1800	55,556
3	2400	41,667
4	3000	33,333
5	3600	27,778
6	6000	16,667

* Note: 16-bit counter overflows because motor speed is too slow.

Based on this simple formula and table, a control scheme can be developed to adjust the duty cycle. We can measure counts between two Hall pulses fairly easily and thus determine whether or not a motor is running at the desired speed. For example, if the desired speed is 3000 RPM, then we should expect 33,333 counts. If we measure 40,000 counts, the motor is running slow and PWM duty cycle must be increased. If we measure 30,000 counts, the motor is running fast and the duty cycle must be reduced.

Code for such control is shown in Figure 17, which again uses an R8C MCU as an example. The timer C peripheral in this setup has two registers, tm0 and tm1. Register tm1 sets up the carrier frequency and tm0 sets up the duty cycle. Output is low (= 0) until the count reaches tm0. When the count matches tm0, the output is turned high (= 1). When the count matches the tm1 value, the output is set low (=0) and the counter is reset. Thus, the active duty cycle extends from the tm0 value to the tm1 value, and the non-active duty cycle is from 0 to the tm0 value.

```

void pwm_set(void)
{
/* set a tm1 register (PWM period) */
tm1 = 1000; //PWM carrier frequency at 20 kHz
case UPDATE_SPIN:
  if(CountMeas > CountRefH)
//If interrupt time is larger than upper limit the pwm increases
  tm0 -= 1; //speed is slower so increase pwm value by reducing tm0
  if(CountMeas < CountRefL) // speed is higher
  tm0 += 1; // so reduce pwm by increasing tm0
    if(tm0 >= 500) // Check for upper limit
      tm0 = 500-1;
    if(tm0 <= 5) // Check for ower limit
      tm0 = 5;
  pwm_upd = tm0;
  break;

tcout = 0x47; /* CMP00-CMP02 enable, CMP10-CMP12 disable */
/* CMP00-CMP02 reverse */
tcc00 = 1; /* timer C count start */
}

```

Figure 17. R8C code in C language for PWM duty control to achieve desired speed.

In our example, the register tm1 is set to a value of 1000 to get a 20 kHz carrier frequency. The time between two Hall pulses is called CountMeas and the high and low reference counts are CountRefH and CountRefL. When time is measured, the value of CountMeas is compared to CountRefH and register tm0 is adjusted accordingly. If the measured count is higher than the reference count CountRefL, the motor is running slow and the tm0 value is reduced to increase the duty cycle. If the measured count is lower than the reference count, the tm0 value is increased to reduce the duty cycle. Finally, a check is made to protect the minimum and maximum values.

Simple code such as this works well for adjusting the duty cycle to get a desired speed. However, in a few cases this control method fails to work properly, particularly, when the increase and decrease in the tm0 register moves back and forth. Recall that we are using CountRefH and CounteRefL—not just a single CountRef—for comparison. This allows us to insert what is known as a dead band. Let’s say that we want our motor to rotate at 3000 RPM. From Table III, we see that the reference count or expected count is 33,333. Now we must apply a dead-band value, which is determined by the accuracy we require. If we require 100-RPM accuracy, then we must compute values for CountRefH using 2900 RPM (34,483) and CountRefL using 3100 RPM (32,258). When RPM gets within this range, the control algorithm will stop adjusting the PWM value. Based on the control frequency, the sensor measurement frequency, and the accuracy requirements, we can tighten this dead-band value. However, we must be cautious. Too tight a dead band will cause the motor speed to fluctuate between one value and another.

Design engineers frequently use proportional-integral control and motor response characteristics to determine gains. This approach generally gives a better control algorithm. We have used such algorithms successfully, but only after we first made the motor rotate closed-loop using the simple approach just described. We generally suggest such an approach.

Starting a motor

Because motors are started in open-loop fashion, they require a duty cycle somewhere between 50 and 70%. This ensures that the motor has enough starting torque and that the rotor will turn in synchronization with the rotating magnetic field of the stator. If the starting torque is insufficient, the rotor may never attain a synchronous state and the firmware may never get feedback from the Hall signals.

Generally motors are started at a 70% duty cycle with a fixed commutation period of about 500 RPM. Once the MCU starts to receive the Hall signals, the speed measurements are stabilized. Then the simple control algorithm stabilizes the PWM value and the speed command is set to the desired speed.

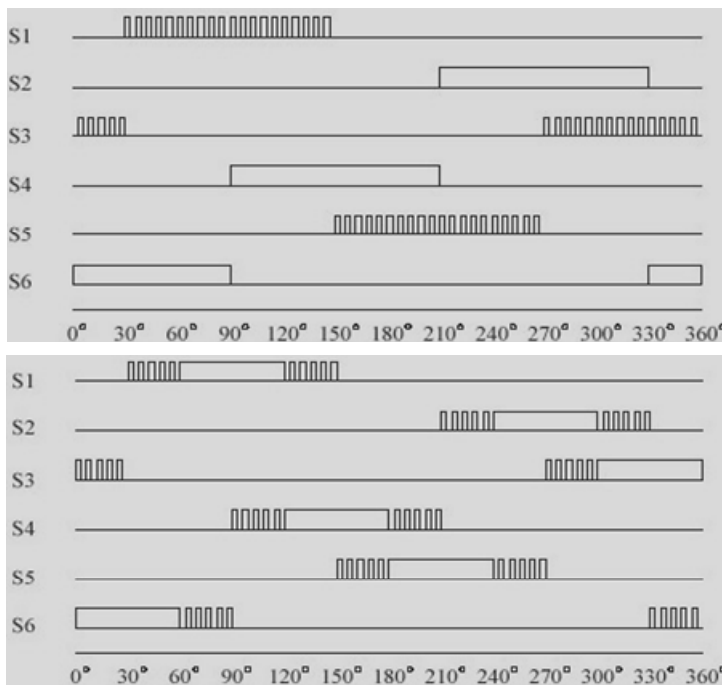
This process works best when we make small, incremental speed changes and allow the algorithm to follow with the appropriate PWM changes.

Modulation schemes

Another issue in speed control is whether to modulate only the Up or both the Up and Vn. Several approaches can be taken. Many designers prefer to modulate only the upper IGBT or power-MOSFET switches, while others choose to modulate only the lower switches. These approaches are known as asymmetric modulation schemes.

If only the upper switches are modulated, then excess energy is drained out of the motor because the lower switches are always on. If only the lower switches are modulated, the motor continues to store energy in the system. The result may be good or bad. Asymmetric modulation creates differing stresses on the switches, so the control algorithm for such modulation has to exactly fit the operation. If the upper switches are modulated, they are subject to greater stress and wear and tear, which increases the probability of their failure.

If only the lower switches are modulated, they will be more prone to failure.



Asymmetric modulation typically employs one of two schemes: 120-degree modulation or 60-degree modulation. As Figure 18 shows, in 120-degree modulation the upper switches are modulated as necessary during the entire on time. In 60-degree modulation, the upper switches are modulated for the first 30 degrees and the last 30 degrees, with the switch left on for the middle 60 degrees. This 60-degree modulation scheme does not permit a full range of operation. In many cases, the motor can be operated only in 50 to 100% of its speed range.

Figure 18 Asymmetric modulation schemes for six step control method.

Some designers modulate both the upper and lower switches. Even though this scheme is somewhat more complicated to implement, it allows more symmetrical stress and wear and tear on the switches. With this scheme, each switch can be modulated 60 degrees at a time, as illustrated in Figure 19, stressing it in a more symmetrical fashion. The scheme also works well with the interrupts and state-change requirements. As we know from the six-step algorithm, a state change is required every 60 degrees. Thus, when a state change is made, a switch is also selected for modulation. As shown in Figure 19, each switch is modulated 60 degrees, creating an equal stress on each. Also, the motor can operate in the full speed range, because the modulation covers the entire electrical cycle. Generally, each switch remains on for 120 degrees of electrical rotation time, and the state-change algorithm selects which 60-degree portion will be modulated.

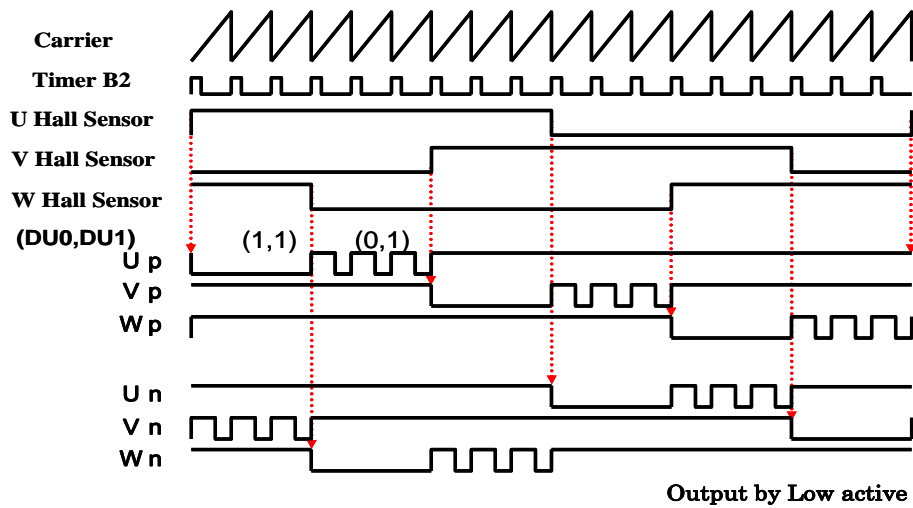


Figure 19. Symmetric modulation scheme that stresses all power switches equally.

If we combine our modulation scheme, speed sensing, and PWM computation within our motor control firmware, then our firmware structure will be similar to that shown in Figure 20 (slide37). Block 1 ensures that proper state changes are made to achieve 120-degree modulation. Many times this commutation is based strictly on the MCU receiving the Hall-sensor signals and processing them in interrupts, an implementation technique that ensures that state changes are made properly. Thus, if the motor is running slowly, no abrupt state changes will be made, and the motor will maintain its synchronization.

Block 2 of Figure 20 has two components, the first of which is used to measure speed from the Hall sensors. This measurement requires the use of a timer resource. For every Hall-signal interrupt, the timer is read and reset so that it will measure the time of the next Hall signal.

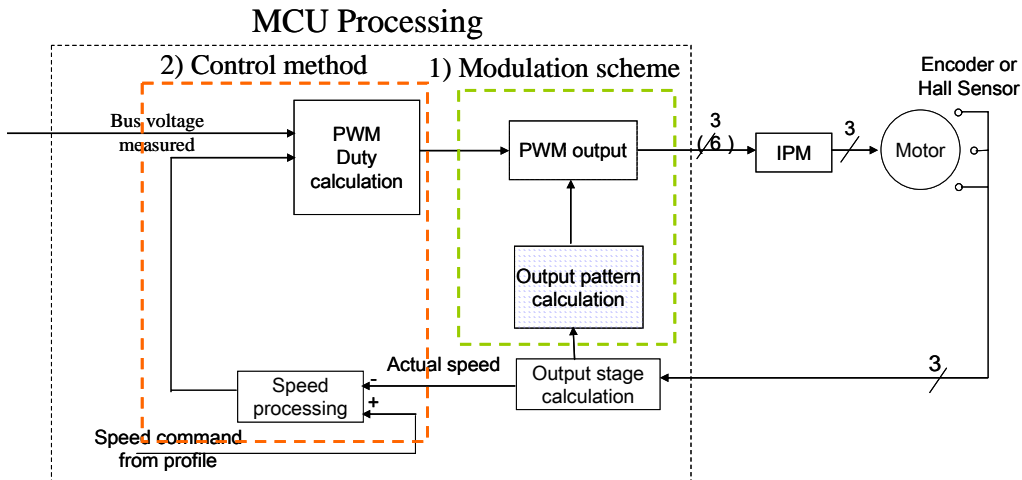


Figure 20. Closed loop control method with position sensor.

The second component in Block 2 uses this measured count or measured speed in the control algorithm to set the new duty cycle according to the calculations discussed earlier. Notice here that we have added a bus-voltage measurement into our scheme. When AC is rectified into DC, voltage ripple can occur at about 60 Hz. Often this ripple is in the 5% range—a large variation that can be handled properly. Because the modulation runs at 20 kHz and the ripple is at 60 Hz, we can correct for the ripple by accurately measuring the bus voltage at the right frequency. Experience tells us that when we make such corrections, the motor will reach the desired speed quickly and maintain that speed properly. If we don't make such corrections, then the voltage ripple will cause torque ripple that may, in turn, cause the speed of the motor to continually vary above and below the set point.

Summary of sensor-based control

Our discussion of BLDC motor control using the 120-degree Hall-sensor method has covered a number of points. To summarize, Hall sensors are an integral part of 120-degree, six-step trapezoidal control. These sensors are used to detect rotor position and to make appropriate state changes (known as the commutation sequence). Using position and timing information, we can measure speed and implement appropriate control. Thus, Hall sensors provide all of the necessary feedback information for the rotor. This method of control has several advantages. It is easy to use, the required code is simple, and switching is straightforward. The switching has built-in dead time and does not require a special timer. Commutation or switching can be directly connected to the Hall signals for simplicity. Moreover, this method implements effective speed control.

However, Hall-sensor based control does have its disadvantages. Hall sensors increase the cost of the motor and require that five more wires be connected. Also, the sensors add another source of EMI to the motor. Their behavior is noisy, too. They are susceptible to corrosion and are usually the first component in the system to fail. If the motor is a hermetically sealed system, Hall sensors will require extra seals.

The 120-degree Hall-sensor control method is reviewed in Figure 21, using an R8C/13 series MCU. Again, the timer C performs the modulation function at 20 kHz frequency. The R8C MCU has an internal structure that allows firmware to multiplex on the output pins as necessary to generate modulation. Firmware can connect the timer C output directly to a pin, or it can disconnect timer C from that pin and set the pin's state to either high or low. That is, the firmware can change the output to high, low, or modulation.

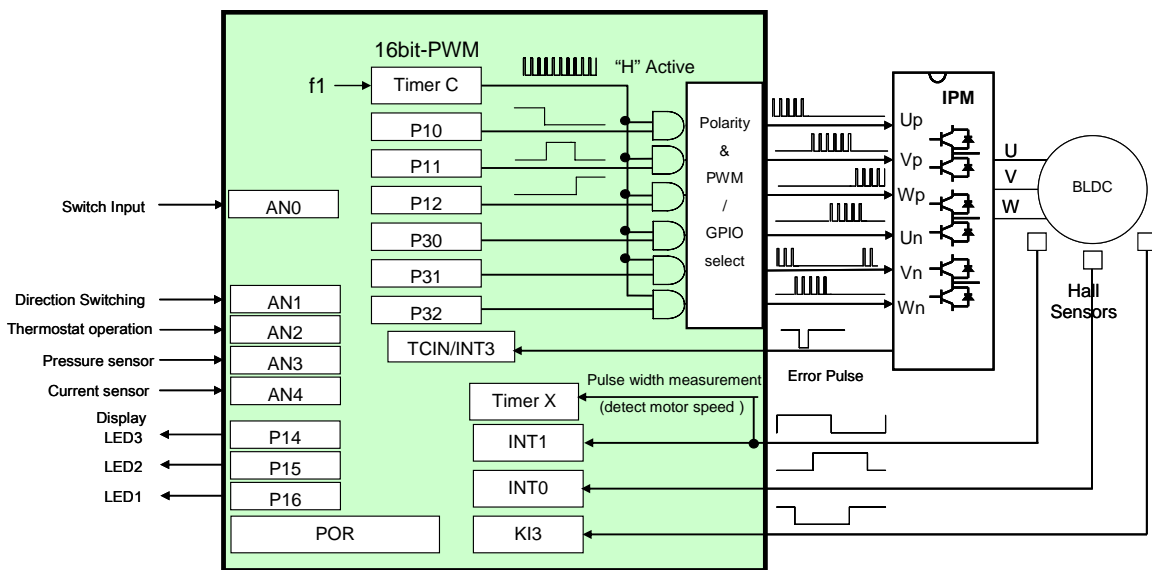


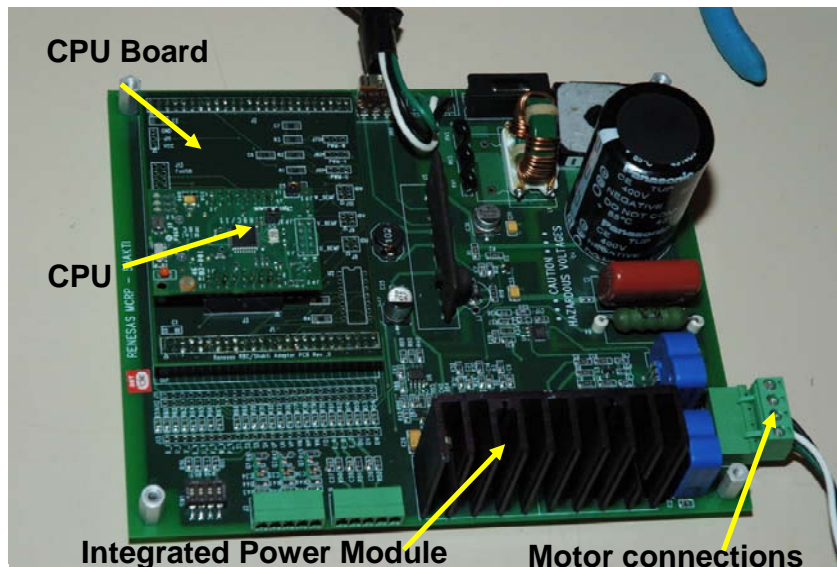
Figure 21. R8C/13 based system configuration for six step control of a BLDC motor.

Looking at Figure 21, notice that firmware also can connect the upper three pins, the lower three pins, or one pin at a time. Six outputs are directed to the integrated power module (IPM), which in turn connects to the three phases of the motor. Three Hall signals are received on three interrupt pins—INT1, INT0, and

KI3—on the rising or falling edges. Timer X, used as the speed measurement counter, measures time between two consecutive Hall signals and provides CountMeas for the speed-control loop. The INT3 pin is used as an emergency-shut-down interrupt when a high-current or a high-temperature alarm signal is received from the IPM.

The R8C MCU has eight ADCs that can be used to implement tasks such as measuring temperature, bus voltage, pressure, and current. Current measurement is particularly important, because measuring average current through several electrical cycles lets us compute torque and speed fairly accurately. By combining speed measurement and current measurement, firmware can determine the point on the torque speed curve at which the motor is operating. Since the R8C MCU has several GPIO pins, the firmware can use an LED on/off scheme to alert us to the internal state of the algorithm and the performance of the motor.

Because the 16-bit R8C MCU runs at a 20 MHz CPU frequency and includes on-chip flash and SRAM, designers can use this device to create single-chip solutions. The MCU's peripherals include eight channels of ADC, three 8-bit timers with pre-scalars, and a flexible 16-bit input-capture and output-compare timer that can generate up to six PWM outputs. The device also has a watchdog timer with ring oscillator, two serial interfaces, a power-on reset function, a low-voltage detect function (generally known as brown-out detect), and an internal clock-generation circuit. Additionally, the MCU has up to 22 I/O pins and 8, 12, or 16KB of flash plus 512 bytes, 768 bytes, or 1KB of on-chip RAM.



Data flash is an especially important feature of the MCUs in the R8C/13 family. The two extra 2KB blocks of data flash have high-endurance write/erase capability and can eliminate the need for external EEPROM for a true single-chip solution. An R8C-based BLDC motor control power board is shown in figure 22 (slide 41) with motor interfaces and IPM placement.

Figure 22. R8C MCU and integrated power module based motor control reference platform.

Sensorless BLDC control

As noted earlier, a significant disadvantage of Hall sensors is their cost. One way to reduce the overall cost of the motor is to eliminate them.

The 120-degree modulation, six-step method of control does allow the use of back-EMF signals to detect the rotor position. Recall that only two of the power switches are turned on at each state change; one is left off. In fact, one entire set of up-and-down switches is not powered on. This is best understood by looking at the Up and Un sequence shown in Table I and also looking at Figure 23.

First the Up switch is turned on for 120 degrees of rotation. Then for 60 degrees there is no power in the U phase. The Un switch is turned on for the next 120 degrees and again, there is no power for next 60 degrees. Thus, every 120 degrees there is a time period of 60 degrees during which we can observe the back-EMF generated by the rotating magnet.

When U_p is energized, current is high in the U coil. When U_n is energized, current is low in the U coil. At this point the current changes direction from positive to negative, thus creating a zero crossing. Detecting a zero crossing is equivalent to detecting the rotor position. However, instead of detecting 60 degrees, 90 degrees are detected. Thus, we can use zero-cross detection to identify the rotor position and then wait until the proper angle is reached to change the state. For example, when a zero crossing is detected at 90 degrees, the firmware can wait another 30 degrees of rotation to perform a state change. The speed-control algorithm remains the same, but a wait period has been added.

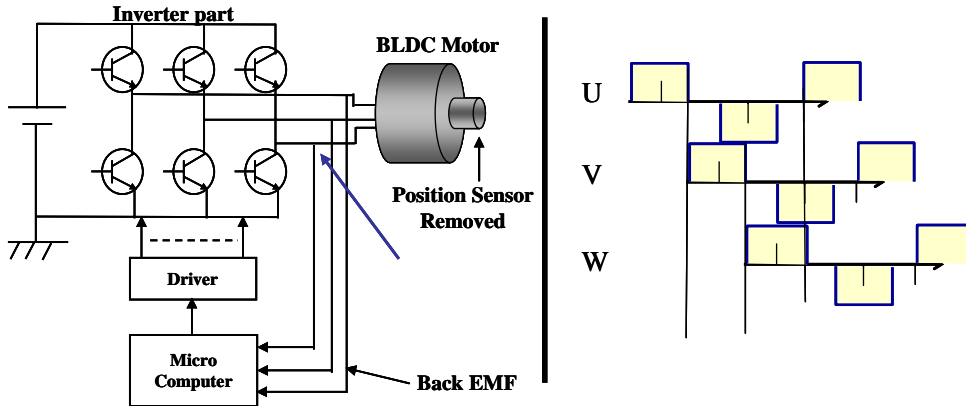


Figure 23. BLDC motor control without position sensor.

Now let's compare the Hall-sensor based algorithm to the back-EMF based algorithm. Both methods use the 120-degree six-step method and perform a state change every 60 degrees. Both methods use the same trapezoidal technique to control speed. The difference between two methods lies in which signal is used for commutation. The sensor-based method uses the Hall signal for commutation. As soon as the signal arrives, the state must be changed. The back-EMF method detects a zero crossing, waits for another 30 degrees of rotation, and then makes the state change. Again, in both methods, the speed-control algorithm and pattern recognition technique are the same.

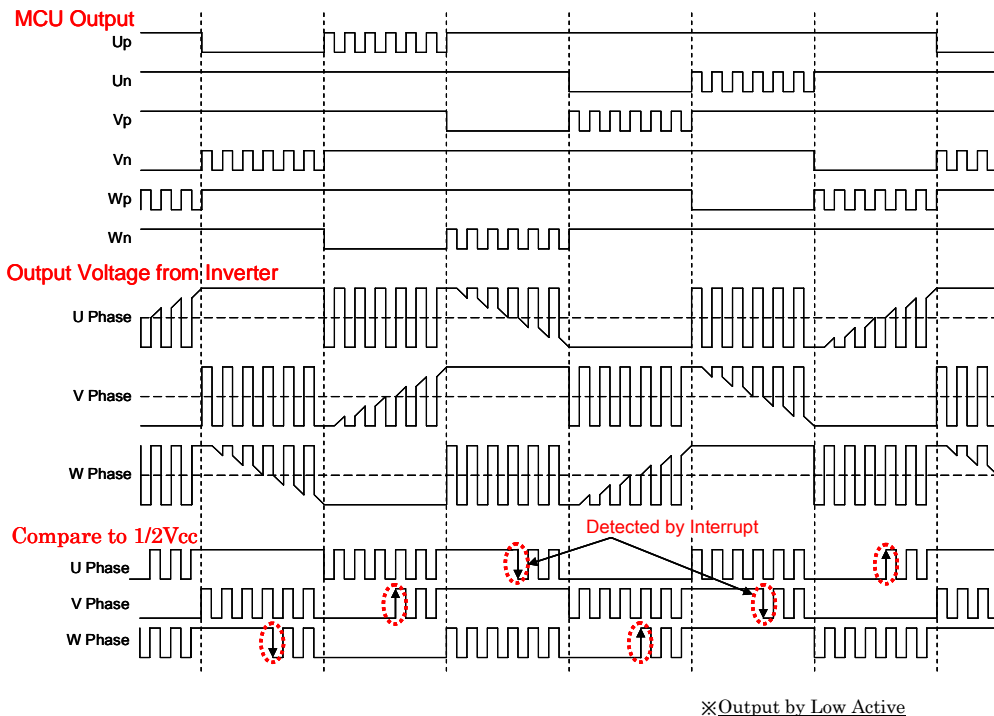


Figure 24. Back EMF detection for symmetric modulation of power switches.

Since both methods use the same type of modulation and the same sequence for energizing phases, both have torque ripple, low efficiency, and high noise. Noise is particularly noticeable when a low carrier frequency is used. The response for speed control is acceptable when the sensor-based algorithm is used, but it is slow for the sensorless algorithm and in some cases inadequate. Further, there are issues with zero-crossing detection. Zero crossing happens in between modulations, when a particular phase is not energized. As Figure 24 shows, the MCU output is modulating each switch 60 degrees. Output for the inverter shows modulation from rail to rail on the voltage. When this voltage is compared to $\frac{1}{2} V_{cc}$, the zero crossing becomes visible and then is detected by the interrupt.

Implementation example

Proper implementation with comparators using an R8C/1A MCU is shown in Figure 25. Back-EMF is detected from the phase voltage, which is high. Thus, a resistor ladder is used to scale down the input into the MCU. Comparators are used to input high or low voltages in interrupt pins as they did in the Hall-sensor example. In this case, when the interrupt is received, the timer X is read and its count is divided by 2. A second counter is then started that will be reset when it reaches one half the timer X count. When that reset occurs, the state change is made. The example shown here uses Timer Y for this purpose. This construct is required because the state change must be delayed for a 30-degree rotation period. Since we have measured the 60-degree rotation time, it's easy to calculate the 30-degree period. Note that because this R8C MCU uses comparators instead of an ADC, it is an extremely cost-effective solution.

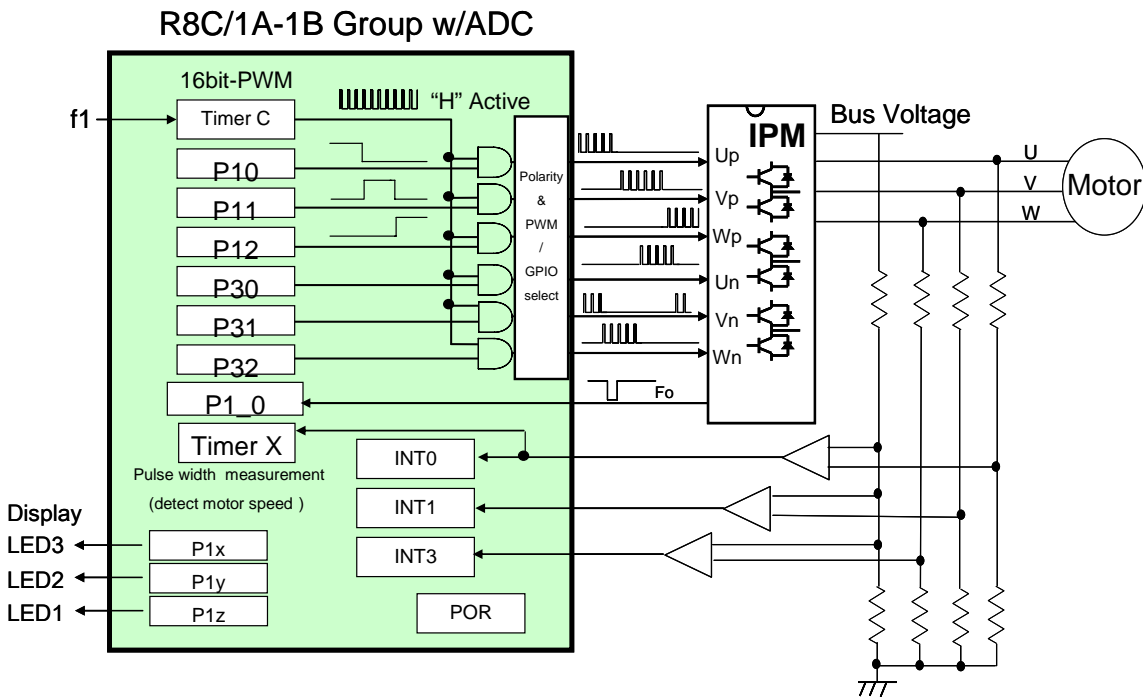


Figure 25. R8C/1A based sensorless implementation with Back EMF detection.

There is little difference between sensor and sensorless control in terms of MCU processing. The pattern calculation and speed processing are essentially the same. See Figure 26 (slide 51). When output stage calculations are done with zero-crossing detection rather than Hall sensors, however, one more timer is required to accommodate the waiting period. This may also change the input masks, which are similar to those used for the Hall 120-degree and 60-degree control methods. Calculations for duty cycle and the bus voltage measurement and corrections are unchanged. Experience shows that proper signal conditioning is required for signals going into the comparators. Otherwise, errors can occur in detecting zero crossings, resulting in poor speed control and high torque ripple.

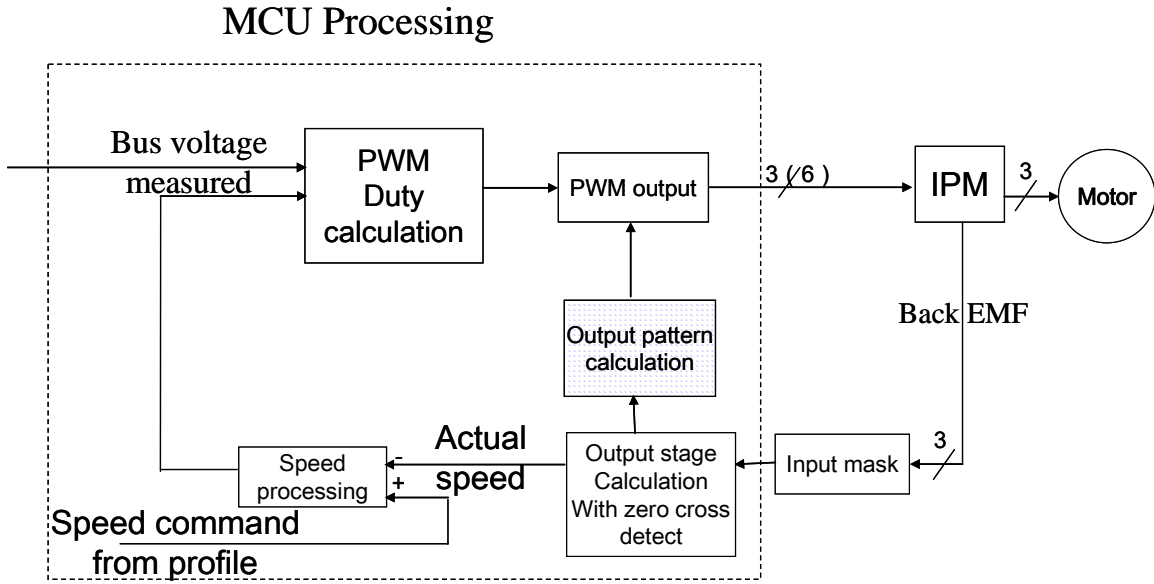
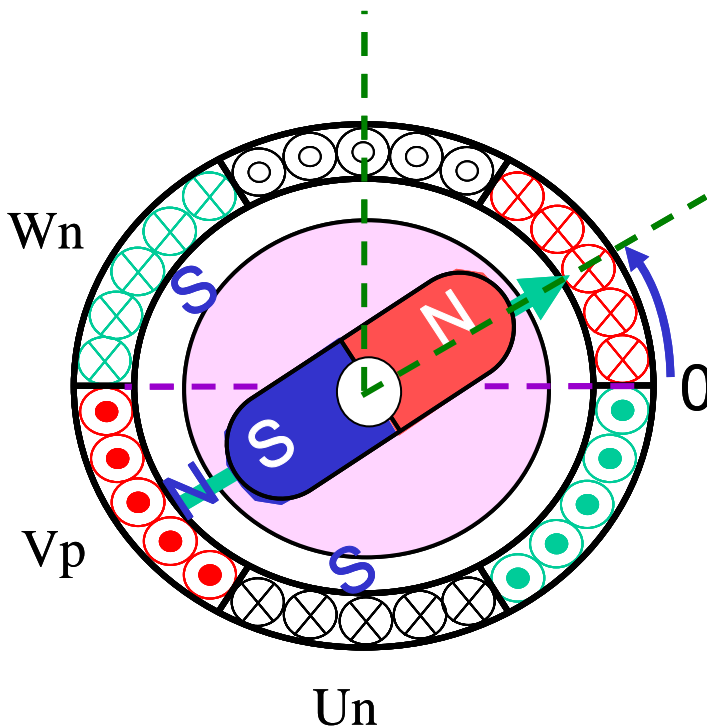


Figure 26. Control flow for sensorless (Back EMF detection) implementation.

Like the Hall-sensor method, the back-EMF based sensorless control approach has advantages and disadvantages. Back-EMF methods eliminate Hall sensors and thus reduce implementation costs. The motor is cheaper to build. However, the cost of new sensors is coming down and decreasing the economic advantage of sensorless motor controllers. Furthermore, sensorless control has various implementation issues. The process of detecting zero crossings introduces extra noise and may cause poor state changes. Sensorless control methods also introduce more torque ripple. Worse, the speed control performance achieved is not acceptable in some applications.

Alignment procedure



It's important to note that before a BLDC motor is commanded to attain a certain speed, its rotor must be aligned properly for smooth operation. This alignment can be done in various ways. One of the simplest is to command the Vp, Un, and Wn for a certain time period, giving a pre-determined number of pulses to the rotor. This procedure aligns the south pole of the rotor with the Vp coil, as shown in Figure 27, which shows a motor that has one pole pair. After the rotor is aligned, it will rotate with a fairly predictable amount of torque, starting with step 1 for a smooth start. The benefit here is that when the rotor is aligned properly, the motor will consume significantly less current during start-up than it would if the rotor had not been aligned.

Figure 27. Aligning the rotor using Vp, Wn, Un coils.

Summary:

We have now completed Part 1 of this seminar. We have covered BLDC fundamentals, the 120-degree commutation sequence and six step-method of rotating the motor, the trapezoidal control algorithm, the Hall-sensor based method of speed control, and the competing back-EMF based method. We have also compared the advantages and disadvantages of these speed-control methods. In the Part-2 seminar we will expand our discussion to cover 180-degree modulation, sinusoidal implementation, open-loop V/f control, and closed-loop control, including CPU bandwidth analysis. We will also provide a quick overview of vector control.

References:

1. **Power Electronics and Variable Frequency Drives Technology and Applications**, Edited by Bimal K. Bose, IEEE Press, ISBN 0-7803-1084-5, 1997
2. **Motor Control Electronics Handbook**, By Richard Valentine, McGraw-Hill, ISBN 0-07-066810-8, 1998
3. **FIRST Course On Power Electronics and Drives**, By Ned Mohan, MNPHERE, ISBN 0-9715292-2-1, 2003
4. **Electric Drives**, By Ned Mohan, MNPHERE, ISBN 0-9715292-5-6, 2003
5. **Advanced Electric Drives, Analysis, Control and Modeling using Simulink**, By Ned Mohan, MNPHERE, ISBN 0-9715292-0-5, 2001
6. **DC Motors Speed Controls Servo Systems including Optical Encoders**, The Electro-craft Engineering Handbook by Reliance Motion Control, Inc. [No ISBN number; very old book.]
7. **Modern Control System Theory and Application**, By Stanley M. Shinnars, Addison-Wesley, ISBN 0-201-07494-X, 1978
8. **The Industrial Electronics Handbook**, Editor-in-Chief J. David Irwin, CRC Press and IEEE Press, ISBN 0-8493-8343-9, 1997

Implementing Embedded Speed Control for Brushless DC Motors

Part 2

Yashvant Jani
Renesas Technology America, Inc.
450 Holger way, San Jose CA 95134
408-382-7716
yashvant.jani@renesas.com

Abstract

Brushless Direct Current (BLDC) motors, also known as permanent magnet motors, are used today in many applications. A new generation of microcontrollers and advanced electronics has overcome the challenge of implementing required control functions, making BLDC motors more practical for a wide range of uses.

This two-part seminar covers BLDC motor control fundamentals and implementation techniques. Part 1 discusses 120-degree trapezoidal control with and without sensors, while Part 2 covers 180-degree sine wave modulation and V/f open-loop and closed-loop control with sensors. Topics discussed include interrupt handling for pulse width modulation (PWM) generation and sensor processing with performance measurement for CPU bandwidth usage. Implementation of a speed profile (speed vs. time) and its interface with the interrupt handler are also described.

Part 2: Introduction

In Part 2 of this seminar, we build on the fundamentals of BLDC motor operation and control covered in Part 1, turning our attention from six-step 120-degree modulation to an examination of 180-degree modulation. We also discuss sinusoidal modulation and look at an example of code used to generate a sine wave. We then discuss open-loop V/f control and closed-loop control. The seminar ends with an overview of vector control.

180-degree modulation

Recall that for six-step 120-degree modulation, power switches are turned on and off so that the current passes through two coils, as shown in Figure 28. Every 60 degrees we switch connections so that the current flowing from coil U to V now flows from U to W. This switching effectively keeps the V coil free of current for the next 60 degrees. During this period when no current flows in the V coil, the back-EMF signal generated by the rotor's magnetic field can be detected in the V coil. The progression of six-step coil energization is shown in Figure 29.

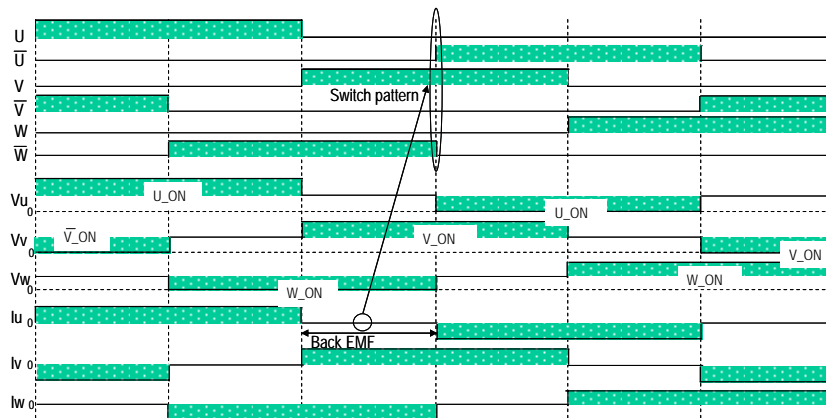


Figure 28. Six steps of trapezoidal control method.

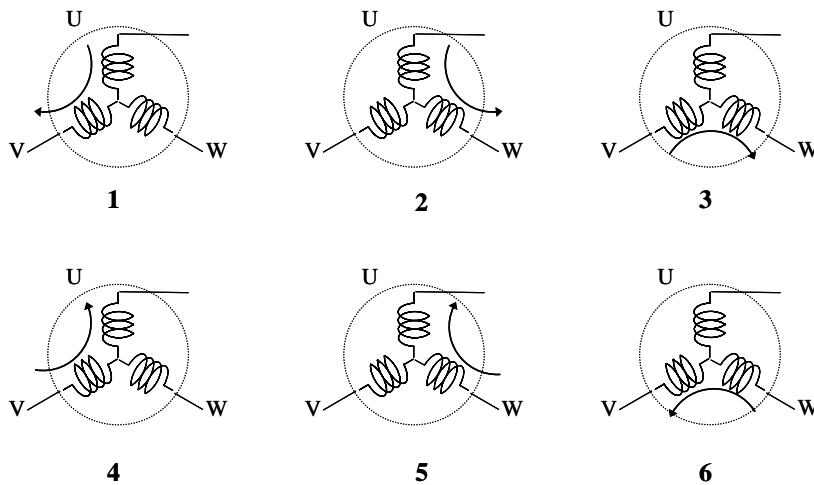


Figure 29. Progression of six coil energization steps.

Another way to understand 120-degree modulation is to look at the timing of U_p , V_p , and W_p during electrical rotation. Each phase is energized for a time that corresponds to 120 degrees of electrical rotation. Phase U_p is on for 120 degrees; V_p is on for the next 120 degrees; and finally W_p is on for the rest of the cycle. Lower switches are turned on and off to provide the path for current flow. In this scheme, there is a period of 120 degrees of rotation in which, for example, phase U does not create any torque on the rotor. Effectively each coil is utilized at only $2/3$ of its capacity.

However, if we could use each coil for the entire electrical period, we would be able to generate more torque on the rotor. So, rather than turning on U_p for 120 degrees of rotation and then waiting another 60 degrees before turning on U_n , what if we could keep U_p on for an entire 180 degrees of rotation with no long wait period before turning U_n on? This modulation scheme is viable, but only if we provide enough transition time between the act of turning U_p off and turning U_n on to protect the switches from a short circuit. If we turn U_n on before U_p has been properly turned off, we risk creating a short circuit that can explode the power switches. The transition time required to safely implement this 180-degree modulation scheme is known as dead time.

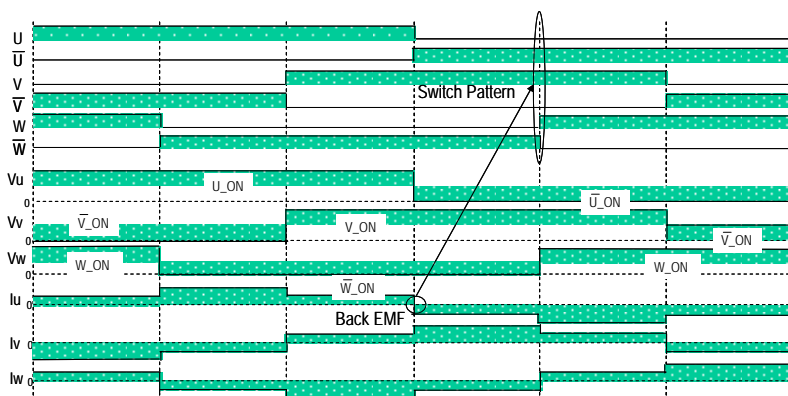


Figure 30. 180 Deg modulation scheme using three coils at a time.

Effectively with 180-degree modulation we are passing the current through all three coils at all times, inserting a small transition time to protect the power switches each time the direction of the current is switched. For the first 60 degrees, current flows in from U_p and from W_p and exits the V_n coil as shown in Figure 30. The W_n coil is no longer free, as it now also passes the current. Next we switch W_p and W_n so

that the current direction changes, and for the next 60 degrees, current flows in from Up and exits the Vn and Wn coils. We continue in a similar fashion for the next four steps. In this way, the coils are utilized fully at all times to create torque on the rotor. Note that the ability to detect back-EMF is greatly diminished because of the short dead time. Generally we say that with 180-degree modulation, there is no back-EMF detection. This statement is correct for all practical purposes. The dead-time requirement also affects the MCU timers, as a dead-time register must be used to insert the proper delay before each phase can be turned on.

We can contrast 120-degree modulation with 180-degree modulation as follows. The 120-degree technique uses only 2/3 of the electrical period to create torque and rotate the motor, whereas the 180-degree modulation scheme uses the entire electrical period. Torque created using 120-degree modulation contains ripples, because torque is applied to a coil for the first 120 degrees, is not applied for the next 60 degrees, and then is applied again for 120 degrees. However, because 180-degree modulation does away with the long (60-degree) wait period, the current flow is smooth and torque ripples are mostly eliminated. Moreover, 180-degree modulation makes possible various other modulation strategies such as sine modulation, quasi-sine modulation, and space vector modulation.

Let's consider the example of a timer with a dead-time register. The Renesas M16C/Tiny series microcontroller unit (MCU) has a special 3-phase timer, shown in Figure 31, which inserts the dead time required between turning the Up and Un power switches on and off. Timer channel B2 generates the carrier frequency and Timer channels A1, A2, and A4 are used with buffers to set the pulse width modulation (PWM) values for on and off counts. The first buffer holds the value that turns on the output when a compare match occurs. The second buffer holds the value to turn off the output on a compare match. When the dead-time register is programmed with a value, two internal signals—P for Up and N for Un—are modified by inserting the dead-time count in the compare match. Then, negative signal N is turned off for Un, dead time is inserted, and positive signal P is turned on for Up. Thus our internal timer hardware makes sure that the upper and lower switches are protected properly.

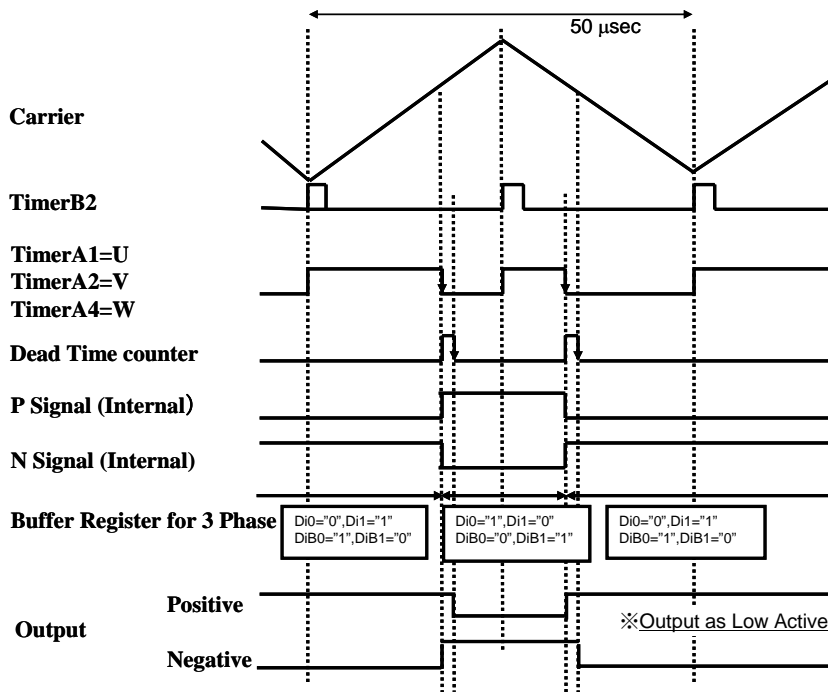


Figure 31. M16C 3-phase timer automatically inserts required dead-time.

The dead-time register is programmed once at the beginning of operation, and the count value is dependent on the characteristics of the power switches. Two internal buffer bits—Di0 and Di1—are programmed to

generate a specific high or low output on the compare match. The compare-match output is high if the bits Di0 and Di1 are set to 0,1. The output is low if these bits are set to 1,0. For the second buffer, the bits are DiB0 and DiB1. By changing the bits properly, a center-aligned or edge-aligned PWM output can be generated easily. Since each channel has a set of buffer bit settings, designers can change the behavior of any channel at will.

The MCU's 3-phase timer is quite versatile in its ability to generate various modulation schemes. It can generate 180-degree, sine wave, quasi-sine wave, space vector, or any custom modulation scheme. It can also generate 120-degree modulation with 60-degree or 120-degree modulation time. It can modulate the upper switches only, the lower switches only, both switches together, or one at a time every 60 degrees. Because the phase timer has dual buffers—the first buffer for the rising-edge compare match and the second buffer for the falling-edge compare match—dual sampling of the angle is possible for better sine-wave generation.

Sine-wave generation

Using the MCU's 180-degree modulation capability, we can generate a sine-wave output easily. In this case, instead of a 360-degree electrical cycle period, we employ a period called the carrier-wave-frequency period. During this period, we calculate sine of the angle and set the PWM accordingly. The basic steps to generate this sine-wave output, illustrated in Figure 32, are as follows:

1. Select a carrier wave frequency f_c such as 20kHz or 16kHz.
2. Select the voltage V_0 and frequency f of the output wave.
3. Compute the phase angle Θ of the voltage at every carrier-wave period.
4. Look up the corresponding sine value from the table.
5. Multiply the sine value with the modulation ratio to generate the PWM value.
6. Transfer the PWM values to the registers.

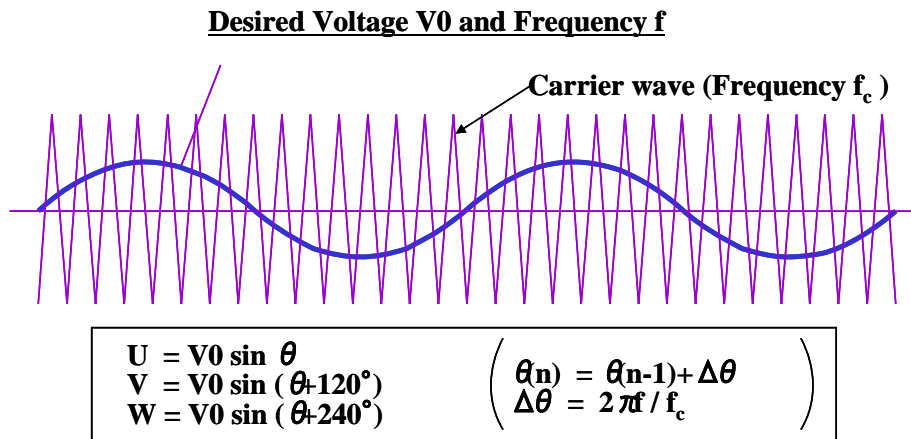


Figure 32. Basic steps of sinewave generation.

The basic formulas are listed below.

$$\begin{aligned}
 \Delta\Theta &= 2\pi f / f_c \text{ (computed once for frequency } f) \\
 \Theta(n) &= \Theta(n-1) + \Delta\Theta \\
 U &= V_0 \sin (\Theta(n)) \\
 V &= V_0 \sin (\Theta(n+240)) \\
 W &= V_0 \sin (\Theta(n+120))
 \end{aligned}$$

Let's examine in detail the steps for sine-wave generation. Three values are required—the carrier frequency f_c , the sine wave frequency f , and the voltage level V_0 . We will use $f_c = 10\text{kHz}$, $f = 50\text{ Hz}$, and $V_0 = 100\%$

of the possible DC bus voltage. The maximum voltage level is V_{dc} and the minimum voltage is zero, thus implying

$$V_{max} = V_{dc} \text{ and } V_{min} = 0.$$

The sine wave is generated from a center value to a maximum value V_0 and then to a minimum value $-V_0$. Therefore the center value is $V_{dc}/2$ computed as

$$(V_{max} + V_{min})/2 = \frac{1}{2} V_{dc}.$$

Note that V_0 (at maximum 100%) is also $\frac{1}{2} V_{dc}$. In our case, $V_{dc} = 160$ volts; therefore, $V_0 = 80$ volts and the center point is also 80 volts. The sine wave is now calculated as

$$\frac{1}{2} V_{dc} + \frac{1}{2} V_{dc} * \sin(\Theta).$$

We can write this as,

$$V_{pwm} = \frac{1}{2} V_{dc} + \frac{1}{2} V_{dc} * \sin(\Theta).$$

We will get $V_{pwm} = V_{max}$ at 90 degrees and $V_{pwm} = V_{min}$ at 270 degrees as expected.

The angle traversed every carrier frequency is now

$$\Delta\Theta = 2\pi f / f_c = 360 * 50 / 10000 = 360 / 200 = 1.8 \text{ degrees.}$$

Also,

$$\Delta t = 1/f_c = 1/10000 = 100\mu\text{s period,}$$

$$\text{Max PWM count} = \Delta t * \text{counting frequency, and}$$

$$\text{PWM max} = \Delta t * 20\text{MHz} = 100 * 20 = 2000.$$

Because we are using a center-edged PWM generation timer, the timer's B2 channel is $\frac{1}{2}$ of this value. The timer B2 period is 1000 counts, and the first PWM for the rising edge is

$$\text{PWM1} = 500 + 500 * \sin(\Theta).$$

We can compare this to

$$\frac{1}{2} V_{dc} + \frac{1}{2} V_{dc} * \sin(\Theta).$$

The second PWM for the falling edge is

$$\text{PWM2} = 1000 - \text{PWM1}.$$

At 90 degrees, the sine of the angle is 1. We must therefore get the maximum number of counts. At 270 degrees, the sine of the angle is -1 and we must get the minimum number of counts.

In summary, to generate a sine wave, we begin with $\Theta=0$ and then set the timer channel B2 to a value of 1000 counts for the count down. We set the interrupt at every second underflow, which is the completion of the triangular center-edge waveform. In the interrupt routine, we compute the angle, look up the sine table, and multiply by the voltage value to compute the PWM1 value. We check this value for maximum and minimum bounds and then compute PWM2. We will examine the code for this procedure in the next section.

You probably noticed that we performed a sine-table lookup in generating PWM. How do we create this sine table? Since the MCU performs all calculations in integer arithmetic, we must use a scaled value for the sine table. We also must use a scaled value for the voltage. Using Microsoft Excel, we can create a sine table with one-degree resolution similar to the one in Figure 33. We start at zero degrees and advance the table by one degree for each entry, using the sine of the average angle for the index. All sine values are computed in floating values, as shown in the third column. We then convert these values to 2^{13} format—that is, value 1 is represented by $2^{13} = 8192$. Next we take the floor value of the calculation to get the sine value in integer format. For the U value, we continue with the angle computation, and for the V and W values, we add a 240-degree and 120-degree offset, respectively, for the lookup process. Then we plot the three values to see if correct sine waves result.

Index	Mid point angle	Sine value	Sine in 2 ¹³ format	Integer value for Sin
1	0.5	0.008726535	71.4877788	71
2	1.5	0.026176948	214.4415605	214
3	2.5	0.043619387	357.3300213	357
4	3.5	0.06104854	500.1096359	500
5	4.5	0.078459096	642.7369122	643
6	5.5	0.095845753	785.1684046	785
7	6.5	0.113203214	927.3607272	927
8	7.5	0.130526192	1069.270567	1069
9	8.5	0.147809411	1210.854696	1211
10	9.5	0.165047606	1352.069987	1352
11	10.5	0.182235525	1492.873425	1493
12	11.5	0.199367934	1633.222119	1633
13	12.5	0.216439614	1773.073317	1773
14	13.5	0.233445364	1912.384421	1912
15	14.5	0.250380004	2051.112993	2051
16	15.5	0.267238376	2189.216777	2189

Three sine waves at a time

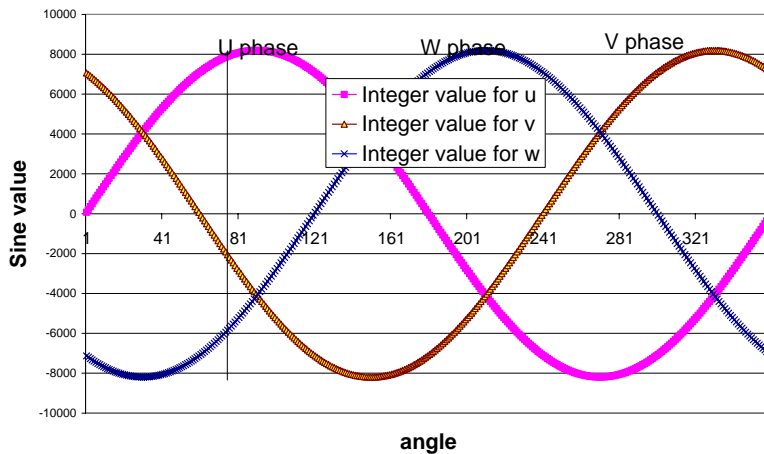


Figure 33. Sine wave table and its graph with integer values.

Several important points should be noted. Applying a dynamically changing PWM voltage to the stator results in sine-wave voltage and current passing through the stator. This action requires a carrier frequency. We select the value of the carrier frequency based on how precise and accurate the applied sine wave must be and how large a table our MCU's memory can handle. Typical carrier frequency values falls in range of 2 to 20kHz. However, many designers want to avoid the audible frequency range, so they select values of or above 16kHz.

Because a single PWM signal cannot create negative current, a lower power switch is used to enable the current to flow in the opposite direction. Positive and negative PWM output switches are required. To protect these switches, dead time must be inserted between positive and negative signals, as we have discussed previously. Hardware-based dead time is more accurate than software based dead time and reduces CPU bandwidth usage.

With sine-wave implementation, we can improve control performance and efficiency. However, this process requires a true 3-phase timer unit with dead time insertion for proper operation. Sine-wave modulation is compared to trapezoidal modulation in Figure 34.

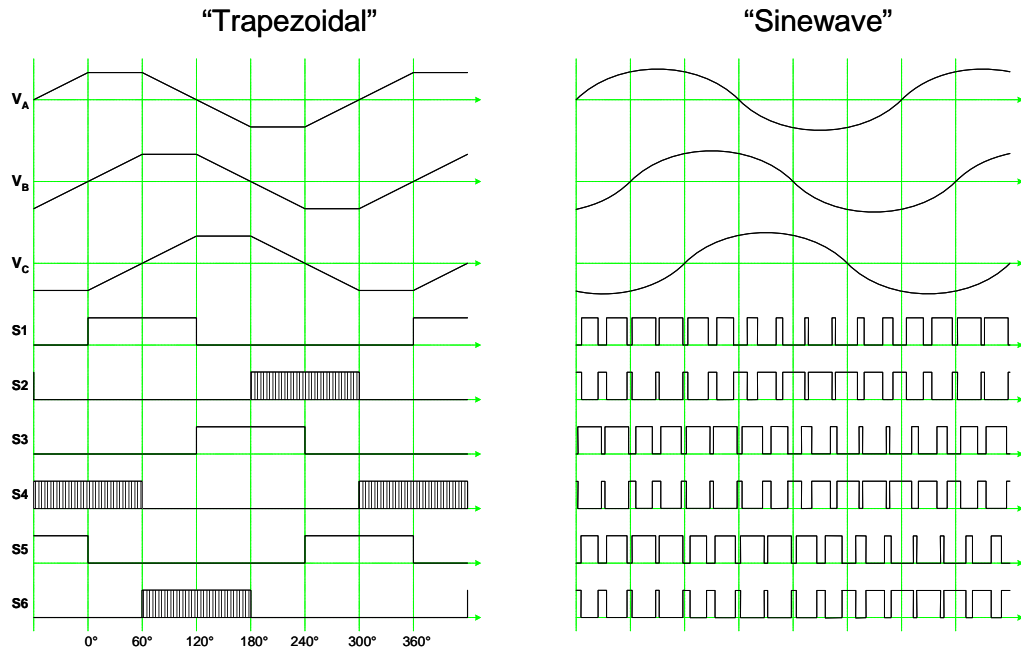


Figure 34. Comparison of 120 deg trapezoidal and 180 deg Sine wave modulation.

Sine-wave generation example

Now let's consider how to code a device for sine-wave generation. We begin with a motor-control reference platform, shown in Figure 35. This platform consists of two boards—a Starter Kit Plus (SKP) and a Power Board. A Renesas M16C/28 series MCU, an LCD, and LEDs are mounted on the SKP. The power board has AC-to-DC conversion and an integrated power module (IPM) with six power switches plus drivers built in. The IPM uses a heat sink, as Figure 35 shows.

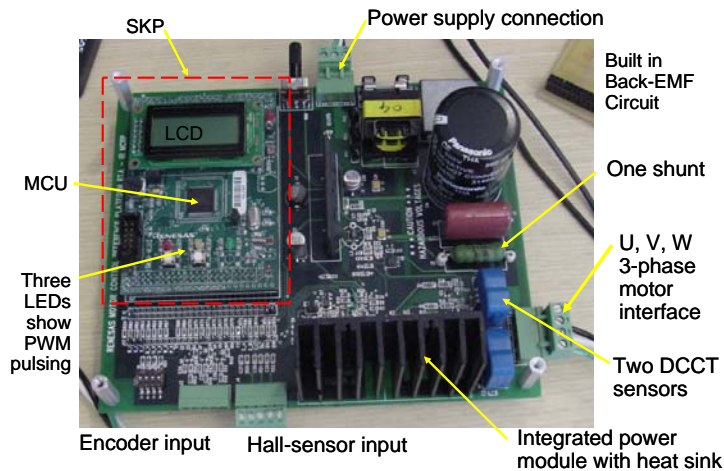


Figure 35. Power and MCU board for controlling the motor.

To measure the motor position and current in the U and V phases, the power board provides a Hall-sensor input, an encoder input, and two DCCT devices. Three back-EMF resistor ladders plus a fourth resistor ladder for measuring the Vbus are also implemented on the board, too. A precision shunt resistor on the low voltage side is also included to measure the overall current or to perform a one-shunt current detection technique for current measurements. Together these elements allow us to run various BLDC algorithms.

Our test set-up consists of a Bodine BLDC motor with two pole pairs, as shown in Figure 36. The MCU is used to generate a sine-wave PWM series of various frequencies, and the current waveforms are captured by the DCCT sensors. (You can view the entire code for the interrupt in Appendix A.) The basic sine wave is generated as follows.

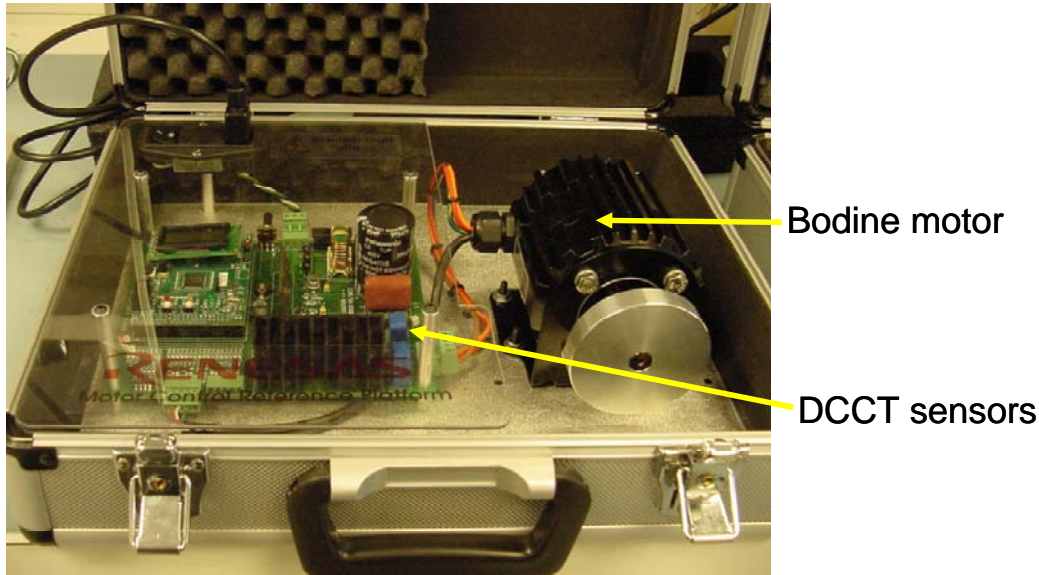


Figure 36. Test set-up with Bodine motor.

When the interrupt is entered, the MCU's firmware checks the validity of the new frequency update. If the update is true, the new frequency is commanded and the delta theta for angle computation is updated. Delta theta is presented in 2^6 format, so **delta theta = 64** means 1 degree, and **delta theta = 96** means 1.5 degree. The firmware then integrates the total angle, denoted as **sinpt_sum**, by adding the delta theta value. If the resulting **sinpt_sum** is greater than 360 degrees (23040 using 2^6 format), then roll-over has occurred and the **sinpt_sum** must be corrected to a new value by subtracting 23040. Then, **sinpt_sum** is scaled back by a 2^6 value to get an index in the sine table. This index is called **sin_pt** in our code.

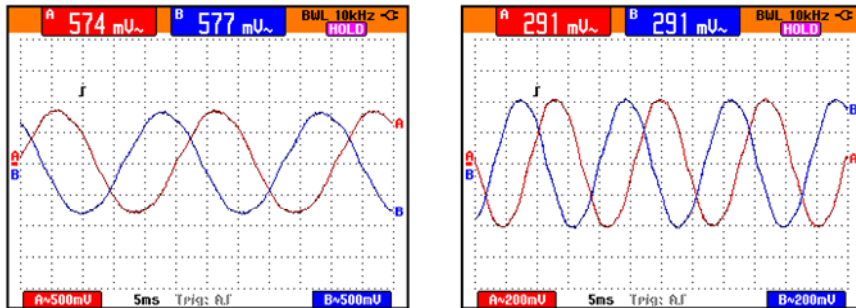
The constants **C4_DAT** and **C2_DAT** in our code are based on carrier frequency and represent $\frac{1}{4}$ and $\frac{1}{2}$ counts for the carrier-frequency time period. For example, assume that the carrier frequency is 10kHz. Thus, the time period is $100\mu\text{s}$. Counting at 20MHz, it represents 2000 counts. It follows that **C4_DAT** = 500 and **C2_DAT** = 1000 counts. Using the **C4_DAT** constant, three PWM values are computed, as shown in Listing 1.

As you can see, **sin_pt** is used as an index for the sine table. Voltage is represented by the variable **tqdat**, and the entire multiplication is scaled by 2^{19} because sine values are given in 2^{13} format and voltage values in 2^6 format. For V and W values, **offset_v** and **offset_w** variables are used. To rotate the motor forward, V and W must have offsets of 240 and 120, respectively. To rotate the motor in reverse, V and W must have offsets of 120 and 240. Notice that this procedure is not unlike running the six-step state table in reverse order.

Listing 1

```
/*U-phase pwm command value = carrier/4 - (sinN° × (torque command value × carrier/4))*/  
pwm_u_w = C4_DAT - (signed int)((((signed long)sin_tbl[sin_pt]*(signed long) tq_dat)>>19);  
  
/*V-phase pwm command value = carrier/4 - (sinN° × (torque command value × carrier/4))*/  
pwm_v_w = C4_DAT - (signed int)((((signed long)sin_tbl[sin_pt+offset_v[direction]]*(signed  
long)tq_dat)>>19);  
  
/*W-phase pwm command value = carrier/4 - (sinN° × (torque command value × carrier/4))*/  
pwm_w_w = C4_DAT - (signed int)((((signed long)sin_tbl[sin_pt+offset_w[direction]]*(signed  
long)tq_dat)>>19);
```

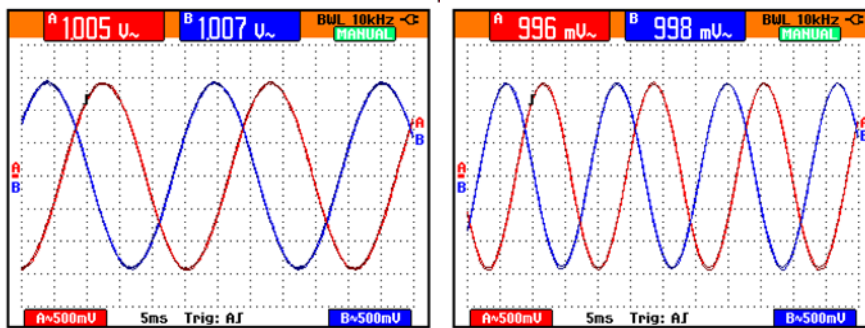
Next, PWM values for U, V and W are checked for PWM_MIN and PWM_MAX to protect the timer operations, and code is developed to reduce the execution time. A PWM2 value is computed using the constant C2_DAT, again to minimize the execution. Finally the six timer registers are loaded, with ta4 and ta41 representing the PWM1 and PWM2 for U phase. Since we have two buffers, we can integrate the angle for the first-half period and use the first index for PWM1. Then we can integrate the angle for the second-half period and use that index for PWM2. Although this method doubles the number of sine lookups and thus increases execution time, it also provides a higher-resolution sine wave.



40Hz Sine Wave

60Hz Sine Wave

Figure 37. Current wave forms using DCCT sensors at 40 and 60 Hz sinewave.



40Hz Sine Wave

60Hz Sine Wave

Figure 38. PWM output with 10kHz filtering.

As Figure 37 shows, we capture the current waveforms at 40Hz and 60Hz using DCCT sensors with 10kHz filtering. As Figure 38 shows, we capture the PWM output from the MCU with 10kHz filtering to view the PWM. We see that the DCCT current waveforms and PWM output are sinusoidal and represent proper fidelity.

V/f open-loop control

Voltage-over-frequency (V/f) open loop control is based on three assumptions:

- 1) Motor impedance increases as the frequency increases.
- 2) A fixed amount of current is most desirable.
- 3) Motor speed can be increased easily by increasing the frequency and related voltage.

Typical V/f control is run from table-based values of for voltage (the tqdat variable in our code) and frequency (delta theta variable in our code), as illustrated in Figure 39. Notice that low frequency values require lower voltage values. Generally a motor has a minimum speed called ω_{\min} and an operational speed ω_{ops} at which the voltage reaches 100%. When the commanded frequency increases beyond the Wops value, the only possible control is to increase the applied synchronous frequency while holding the voltage level steady at 100%. Table values from Wmin to Wops, as plotted on the chart in Figure 39, are determined in the laboratory by observing the current, which is generally kept constant. When the frequency increases beyond the Wops value, the current value decreases. Most of this decrease in current comes from the generation of back-EMF current by the rotating magnetic field. At Wmax speed, current becomes minimal. Generally we do not drive the motor beyond this maximum speed.

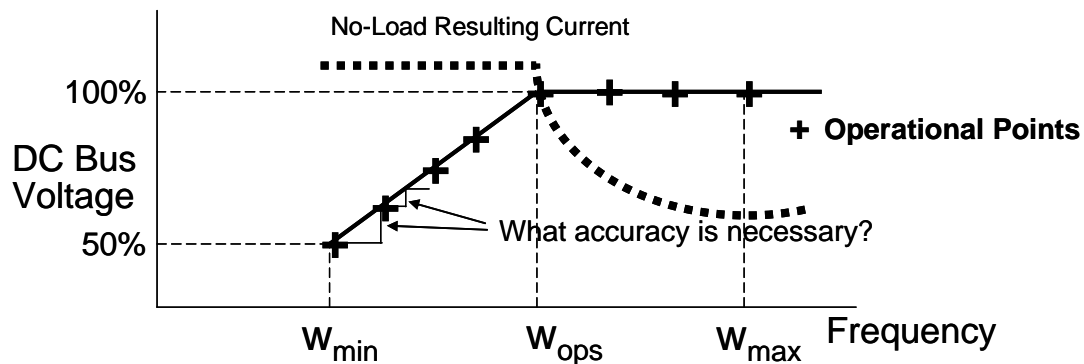


Figure 39. V/f open loop control with current behavior and operational points.

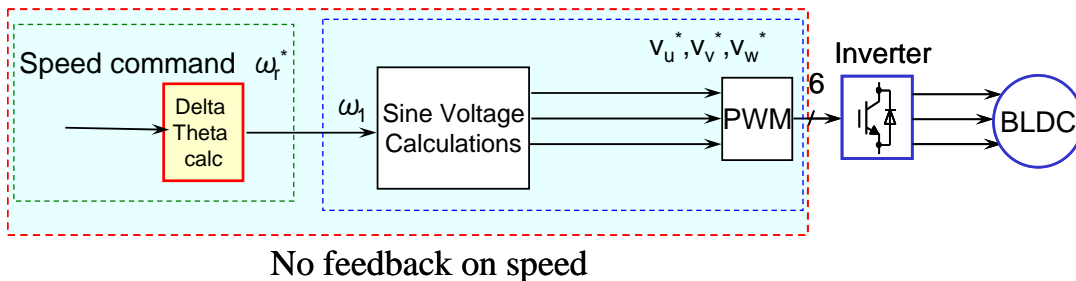


Figure 40. Firmware flow for open loop V/f control without any speed feedback.

V/f open-loop control, illustrated in Figure 40, starts with a desired motor speed. Firmware looks up the table values to set the command frequency and pre-determined voltage level. The timer is initialized and three sine waves are generated at the commanded frequency and voltage level. An interrupt routine handles the sine wave generation using PWM values. No feedback is given regarding the motor speed; we assume that the motor is running at the speed desired. This type of control is known as open-loop control—no closed loops whatsoever are used. Generally, Wmin and Wmax depend on the motor plus load and Wops is determined by the system configuration.

This control method has two main advantages. First, it requires no measurement of current or speed. Second, it uses a simple algorithm that is easy to implement. With some experimentation, we can rotate any BLDC motor without knowing the details of its parameters. This simplicity, however, also has its disadvantages. Without feedback, we do not know at what speed the motor is running. If the load is variable, the motor speed will be variable also. If the system requires some form of speed control, a speed sensor can be added. However, this moves us to a closed-loop control system.

The open-loop method provides no reading of the current, so an overcurrent condition is possible. To protect against this condition, a shunt current resistor can be used to measure the steady-state current. This technique gives some feedback regarding speed as well as overcurrent. It may also give some feedback about the load on the motor. Adding a shunt current resistor is relatively easy and again moves us to a form of closed-loop control.

Open-loop implementation example

In Figure 41 we have implemented open-loop control to show a profile with three-speed motor operation. We start the speed profile at 5 seconds by commanding a low speed of 2400 RPM. We use a ramp in speed, shown in Figure 42, to reach the commanded speed and we also use a ramp in voltage. We begin generating a sine wave with a commanded value of 1200 RPM (20Hz) and voltage (torq) value of 50% (32), because voltage is scaled 100% using a 2^6 format. During the interrupt processing, we create a “near zero” flag when the angle (or sin_pt) is near zero. In the main routine, when the near zero flag is true, firmware changes the commanded speed by a small amount—for example, 120 RPM—and also increases the torq value by 1. Based on the speed and torq start and stop values, different ramp profiles will be generated.

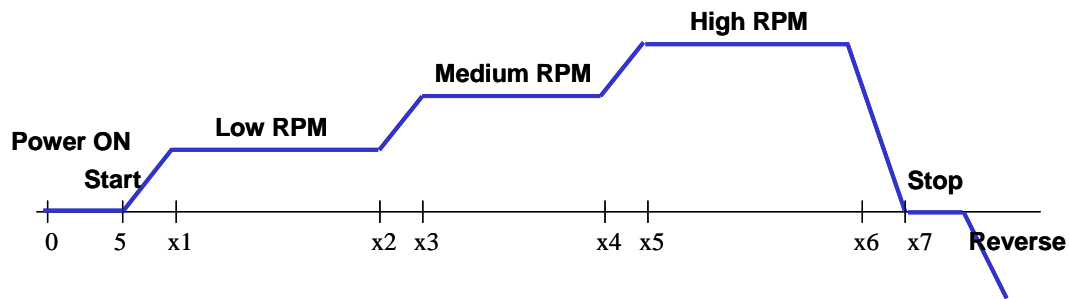


Figure 41. Speed profile with three different speed values as a function of time.

Speed Ramp based on 10 cycles change

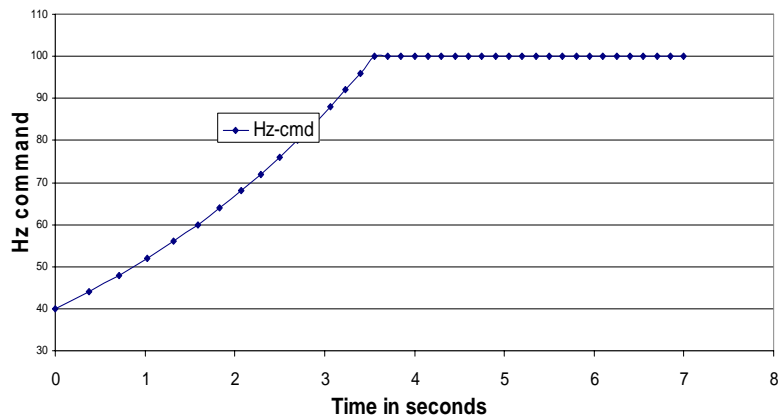
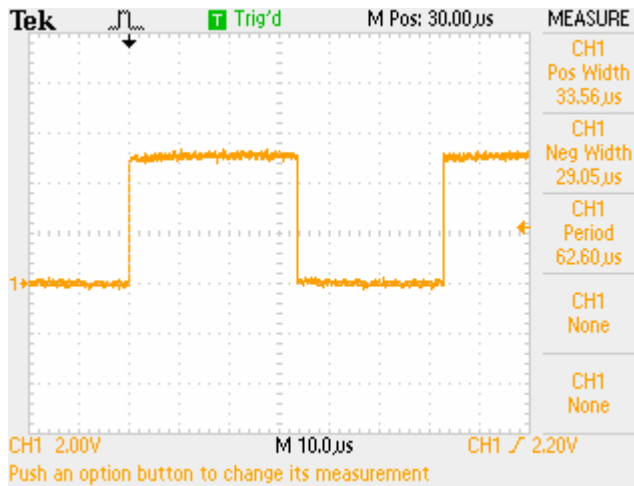


Figure 42. Speed ramp from 40 to 100 Hz as a function of time.

The motor is run at low speed for 60 seconds and then the speed is increased to a medium value of 3000 RPM. The motor reaches medium speed using the same ramp module. Then the motor is run for an additional 60 seconds and the commanded speed is increased to its high speed value of 3600 RPM. We run the motor for 60 seconds at high speed, then slow it down to 1200 RPM and stop it. We wait for 5 seconds, change the index offset, and start the motor again. This time we run the motor in reverse—an important step, because we want to be sure that the motor has this ability.



Within the interrupt code, we use a port pin to output high (1) and low(0) state. When we enter the interrupt processing module, we output high (1) state on this port pin. When the interrupt processing is complete, we output low (0) state on the pin. In this way we can measure the CPU bandwidth, as Figure 43 shows. The rising-edge to rising-edge time is our carrier-frequency time period, and the rising-edge to falling-edge time is the time it takes the firmware to execute the interrupt-processing routine.

Figure 43. CPU bandwidth measurement for open loop sinewave.

Figure 43. CPU bandwidth measurement for open loop sinewave.

At a 16kHz carrier frequency, the measured interrupt time is 62.60µs, whereas the calculated value is 62.50µs. Our result is within the measurement error. The execution time is measured as 33.56µs, which gives us a CPU bandwidth usage over 50%. Thus more than half of the available CPU processing time is used in this interrupt. However, interrupt processing is the only time-critical task that the CPU has to do in this open loop implementation. Although not ideal, our open loop implementation is reasonable because it leaves about 50% of the CPU's time for performing other non-critical tasks. For closed loop, we will need to add other time critical tasks that will require us to reduce the CPU bandwidth for sine wave generation task.

Optimizing the sine code

Our next step is to optimize the code for sine wave PWM execution time for three reasons. 1) If we want to increase the carrier frequency from 16kHz to 20 or 25kHz, then, the interrupt time is 50 and 40 µs respectively. In this case, the CPU bandwidth usage will be 66% and 80% which is generally not acceptable. 2) We want to add time-critical speed and current measurement tasks, and 3) We want to add interrupt driven closed loop control code, which is a time-critical task also. Therefore, it is better to reduce the Sine wave PWM execution time early. To improve performance, we'd like to reduce the CPU bandwidth usage from its current level of over 50%. First we measure individual times for each PWM computation, including table lookup and long multiplication. We are looking for ways to avoid table lookups because they take a lot of time. A significant amount of time is also being spent in MAX-MIN checking. If we can avoid some of this computation, we will save more CPU bandwidth. After detailed analysis, we implement the following changes in our code:

1. Instead of computing the sine value for W index, we simply use the sum of the U and V sine values. This is true for one case only: when all three sine waves are 120 degrees apart. If the index difference between U, V, and W is not 120 degrees, then such replacement cannot be made. Since this technique is applicable to our implementation, we now save the time required for table lookup, long multiplication, and scaling.

2. We study the upper and lower bounds of the table as well as the torq voltage variable in our code and guarantee by design that the PWM values generated by our equations will not require MAX-MIN checking. Then we eliminate these checks. This process saves more CPU bandwidth but requires that we spend time reviewing the entire code for such a guarantee.
3. Finally, after making sure that we have generated a proper sine wave, we turn on the compiler optimization flag.

The optimized code is shown in Listing 2. Running this optimized code, we measure the CPU bandwidth again for comparison. As Figure 44 shows, the CPU interrupt-processing time is now $14.31\mu\text{s}$, down from $33.56\mu\text{s}$ required for the original code. This is a reduction of more than 50% and thus CPU bandwidth usage is significantly lower. For a 16kHz carrier frequency, interrupt time is now $62.5\mu\text{s}$, which translates into 22.9% CPU bandwidth usage versus 53.7% with the original code. These improvements give firmware designers the freedom to add time-critical sensor measurement and closed loop control tasks that are useful in motor control.

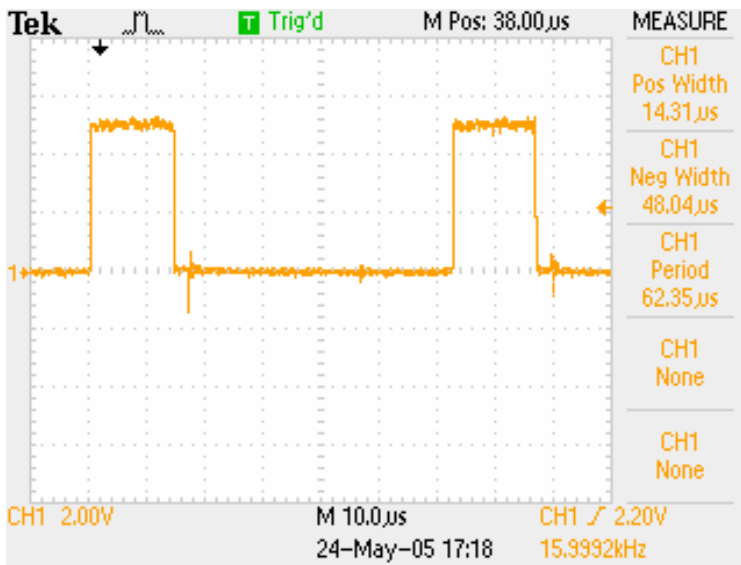


Figure 44. CPU bandwidth for optimized code.

Listing 2

```
#pragma INTERRUPT/B tb2_int
void tb2_int(void)
{
    static unsigned int dTheta;
#ifdef TIME_PWM
    p7_0 = 1;
#endif
    if(Update) {
        dTheta = DeltaTheta;
        Update = FALSE;
    }
    sinpt_sum = dTheta + sinpt_sum; /*Sine pointer sum .. sine skip-read value + sine
pointer sum */
    if(sinpt_sum > 23040) { /*Sine pointer sum max. value? 23040 = 360° x 64 */
        NearZero = TRUE;
        sinpt_sum = sinpt_sum - 23040; /*Sine pointer sum max value revision sin*/
    }
    sin_pt=sinpt_sum >> 6; /* sine pointer sum / 64 */
/*U-phase pwm sine value = (sinN° x (torque command value x carrier/4))*/
    pwm_u_w = (signed int)((((signed long)sin_tbl[sin_pt]*(signed long) tq_dat)>>19);

/*V-phase pwm sine value = (sinN° x (torque command value x carrier/4))*/
    pwm_v_w = (signed int)((((signed long)sin_tbl[sin_pt+offset_v[direction]]*(signed
long)tq_dat)>>19);
/*W-phase pwm Sine value = (sinN° x (torque command value x carrier/4))*/
    pwm_w_w = -(pwm_u_w + pwm_v_w);// - C4_DAT;
/* deleted the checks on MAX and MIN -----*/
    ta4 = (unsigned int)(C4_DAT - pwm_u_w);
    ta41 = (unsigned int)(C4_DAT + pwm_u_w);
    ta1 = (unsigned int)(C4_DAT - pwm_v_w);
    ta11 = (unsigned int)(C4_DAT + pwm_v_w);
    ta2 = (unsigned int)(C4_DAT - pwm_w_w);
    ta21 = (unsigned int)(C4_DAT + pwm_w_w);

#ifdef TIME_PWM
    p7_0 = 0;
#endif -----
}
```

Closed-loop scalar control

Since we have optimized the sine-wave implementation, let's now investigate closed-loop control using a scalar formulation. Closed-loop control requires some type of position sensor that can measure speed, as shown in Figure 45. We can get the required position feedback from a single Hall-sensor that gives one pulse per mechanical rotation, a tachometer sensor that outputs eight pulses per mechanical rotation, or from a Hall commutator that gives six signals per electrical rotation.

An input-capture function coupled with the proper counter provides two measurements: elapsed time from one input capture to a second input capture, and change in rotor position. Both measurements together provide the speed measurement. As we can infer from Figure 45, the rotor position can be detected at every input capture, and using the previous input capture data, the speed of the rotation can be computed.

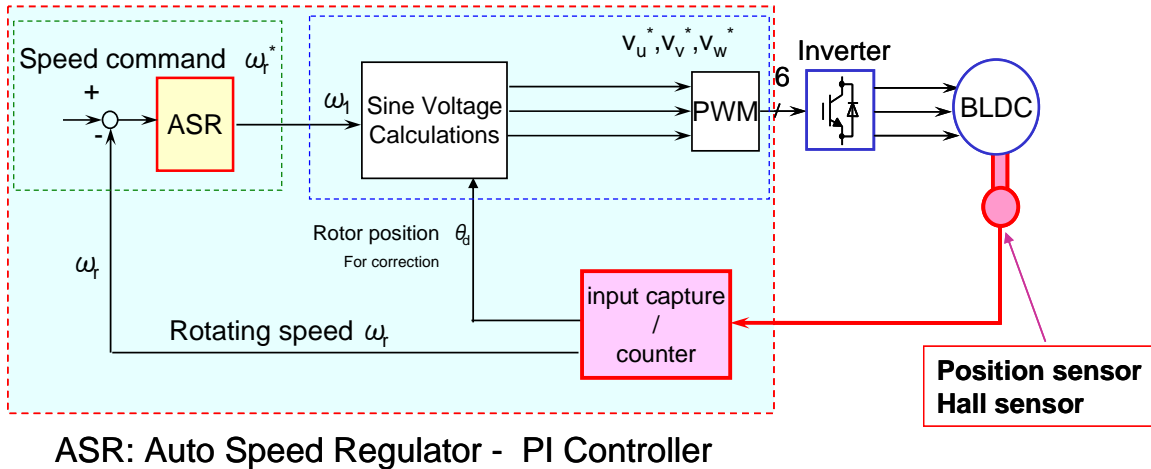


Figure 45. Closed loop speed control using position sensor and input capture timer.

Since we obtain the desired speed or speed command from a pre-set profile, it is easy to implement a proportional-integral (PI) speed regulator as shown below.

$$\Delta\omega_1 = K_p * (\omega_r^* - \omega_r) + K_i * \Sigma (\omega_r^* - \omega_r)$$

Where ω_r^* = speed command,
 ω_r = speed measured,
 K_p = proportional gain,
 K_i = integral gain, and
 Σ is the sum over pre-determined range.

Then, the new speed or frequency ω_1 for sine-wave generation is $\omega_1 = \omega_{1p} + \Delta\omega_1$, where ω_{1p} is the previous value of the same parameter.

A similar algorithm is deployed for the new voltage value of the sine wave. Thus, two parameters are computed for each speed measurement: a new sine frequency and a new sine voltage. In many designs, voltage calculations are not implemented because the motor at that point is already running at the operational voltage and there is no need to change it. In such cases, eliminating the voltage calculations saves CPU bandwidth.

Another form of control is based on the proportional-integral-derivative (PID) algorithm. In this method, a derivative term is added to the equation using the change in the error term.

$$\Delta\omega_1 = K_p * (\omega_r^* - \omega_r) + K_i * \Sigma (\omega_r^* - \omega_r) + K_d * \{ (\omega_r^* - \omega_r) - (\omega_r^* - \omega_r)_p \}$$

Where $(\omega_r^* - \omega_r)$ = error in speed,
 $(\omega_r^* - \omega_r)_p$ = previous value of error, and
 K_d = derivative gain.

Other terms remain the same. This method offers excellent control of acceleration and braking and is preferred by many experts. Disadvantages of PID, however, are convergence time and stability of the control. Depending on the gain values, the PID algorithm may react to small changes and continually perturb the system performance. Based on his experience, the author prefers to implement PI type control.

Hall processing

Let's take a look at the sensor processing steps and CPU time necessary to implement closed-loop scalar control. We use a single-pulse-per-rotation Hall-sensor for this implementation. A free-running, down-

counting timer is started during initialization. Then, at every Hall interrupt, this timer is stopped and the counts are moved into a variable called **New_Meas**. The timer is reset or reloaded and started again. A flag called **new_data** is set for the next task.

When the new_data flag is set, the **process_hall** module computes the speed. The module checks for conditions such as underflow or overflow and then calculates speed, based on one pulse per rotation. If we have implemented the type of Hall-sensor generally used for commutation signals, then speed is computed based on 60 degrees of electrical rotation. Next, the speed computation is converted into mechanical speed using proper transformation based on the number of pole pairs. The new_data flag is cleared for the measurement task and a flag is set for the speed regulator, which we call the velocity regulator. Once the new flag has been set, the velocity regulator processes the new speed measurement and creates new values for frequency and voltage using one of the formulas previously described.

Running closed-loop control of our BLDC motor using Hall sensors and other sensors gives preliminary measurement results such as those shown in Figures 46. The execution times for the two tasks are as follows:

Process_halls	16μs every Hall interrupt
Velocity_regulator	10μs every speed measurement → every Hall interrupt

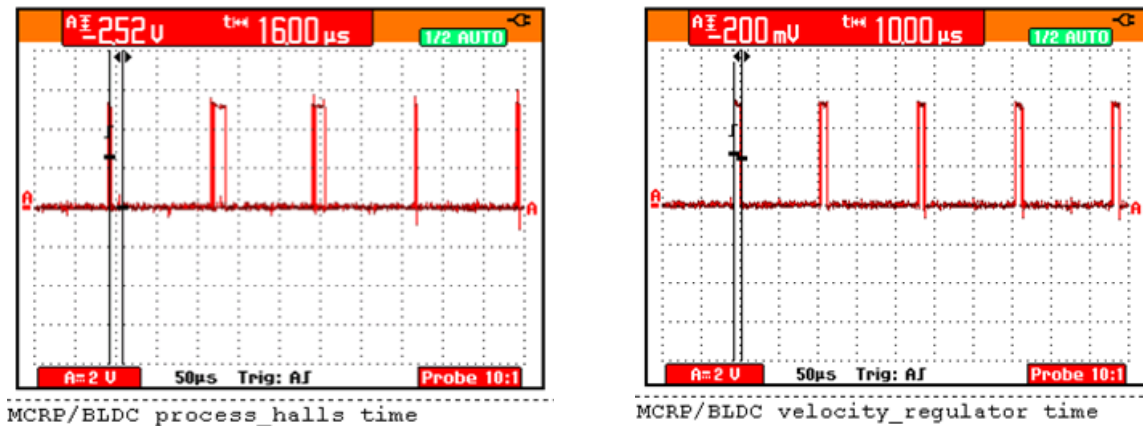


Figure 46. CPU bandwidth measurements for sensor measurement and closed loop speed control.

Now we'll analyze CPU bandwidth usage for this closed-loop control. Sine wave PWM interrupt processing time is 15μs. At a 16kHz carrier frequency, this time is 16000*15, which gives an interrupt-processing time of 240000μs. This time period, which is required to generate a proper sine wave at a given frequency, represents nearly 24% of the CPU bandwidth at the 16kHz carrier frequency. Note that the sine wave PWM interrupt-processing execution time is not dependent on the speed. This is good news, because firmware designers will not have to calculate CPU loading every time the speed changes. The CPU usage turns out to be nearly constant at every speed.

Our execution time for speed measurement or Hall process is 16μs. Let's use the case in which one Hall signal is sensed and processed per rotation. Because the number of times Hall processing must be performed depends on the speed of the motor, the processor bandwidth required for speed measurement will also be speed dependent. We will create a table, called Table IV, for two different speeds. Note that velocity- or speed-regulator execution time is 10μs, and is also speed dependent. This measurement also has an entry in our table. We compute the CPU bandwidth for two speed values—100Hz and 200Hz (indicating that each task must be processed 100 and 200 times). As shown in the last column of Table IV, the CPU bandwidth increases very slightly, from 24% to 24.2% and 24.5%. That is not much of an increase at all.

Table IV. CPU Bandwidth calculations for one sensor measurement and one control processing per mechanical rotation

Speed (RPM)	Speed (Hz)	Hall Process time in μs	Velocity regulator time in μs	Total time
6000	100	1600	1000	242600 μs or 0.24 seconds
12000	200	3200	2000	245200 μs or 0.245 seconds

We also want to calculate the CPU bandwidth for a case in which typical Hall commutation signals are used for speed measurements. Our motor has four pole pairs, and thus four electrical rotations per one mechanical rotation. Since there are six commutation signals per electrical rotation, the number of Hall processes has now increased by a factor of 24. We average the speed measurements for one electrical rotation and apply the velocity regulator once per electrical rotation or four times per mechanical rotation. The corresponding CPU bandwidth calculations are summarized in Table V.

In this case, sine-wave generation requires the same bandwidth as before, while speed measurement and speed control is done more often and therefore require more bandwidth. However, the increase in CPU bandwidth is still not much: bandwidth usage increases from 24% to 28% and 32 %, which is an increase of only about 4% for every 6000 RPM increase.

It's important to point out that we made our calculations to show how the CPU bandwidth usage increases. The designer must still decide how to set the speed measurements and control-loop timings. If other tasks will be impacted by the 4% bandwidth increase, perhaps they can be scaled back. This kind of tweaking may have an impact on speed accuracy, but that is what optimization is all about. As we saw previously in Table IV, we can always perform speed measurement and speed control tasks only once per mechanical rotation to reduce the CPU bandwidth.

Table V. CPU Bandwidth calculations for 4-pole-pair motor.
(24 times sensor measurement and 4 times control processing per rotation.)

Speed (RPM)	Speed (Hz)	Hall Process time 24 times per mechanical rotation	Velocity regulator time in μs 4 times per mechanical rotation	Total time
6000	100	38400	4000	282400 μs or 0.28 seconds
12000	200	76800	8000	324800 μs or 0.32 seconds

V/f open-loop control versus closed-loop scalar control

We have discussed in detail the methods for V/f open-loop and closed-loop-scalar control and evaluated the CPU bandwidth requirements for each. Now let's compare features and benefits of each type of control method. As the name implies, V/f open-loop provides no feedback regarding speed, while closed-loop control performs speed measurement using some sort of position sensor—for example, commutation Hall-sensors; a single Hall-sensor; an encoder with A, B quadrature and Z zero synch pulses; or a tachometer with multiple pulses per rotation.

In both the open- and closed-loop methods, the MCU generates sinusoidal modulation to the inverter drivers. However, speed-control accuracy differs significantly. Because the open-loop method does not provide either feedback correction or control of the speed, the accuracy is poor. With closed-loop scalar control, on the other hand, the feedback on actual speed and the corrections made to the frequency and voltage generation result in highly accurate speed control. The motor rotates very close to the commanded

speed in scalar control. No such expectation is possible in open-loop control, though, which cannot even tell us at what speed the motor is running.

Torque control is not applied in open-loop control, and it exists only indirectly in scalar control.

In terms of MCU resources, both control methods require a three-phase timer unit with dead-time insertion capability. Open-loop control requires no further resources except monitoring for high current and high temperature conditions that would call for emergency shutdown. In scalar control, however, the MCU must have an additional timer to measure the time between two position pulses, as well as input capture with interrupts. The V/f open-loop control method is relatively easy to implement at minimal cost, while the need for sensors makes scalar control somewhat more expensive.

Vector control

Another method worth discussing is vector control. The detailed formulation of this method to control the torque and flux in PMSM was originally achieved by Jahns, Kliman, and Neumann [1] in the mid-1980s. Additional work has been done by many authors, and you will find more information and explanation in references [2,3,4]. Here we will simply summarize the concept and compare it to the 180-degree V/f open-loop and closed-loop scalar control methods previously discussed.

When we examine the torque equation for a brushless DC motor, we realize that the equation is really a vector formulation with the vector product of the current and magnetic fields shown on the right-hand side:

$$\mathbf{T} \rightarrow \mathbf{I} \times \mathbf{B}, \text{ where current and magnetic field are vector quantities.}$$

If we formulate a rotor frame that has a d-axis parallel to the north-south line and a q-axis perpendicular to the d-axis, as illustrated in Figure 47, we can actually convert the stator currents in the rotor frame. We then realize that the current along the d-axis creates pure flux, whereas the current along the q-axis creates pure torque. Denoting these two currents as I_d and I_q , we can say that our control algorithm must control both these currents to maintain proper flux and proper torque in the system. We know that speed is directly related to torque, and torque is related to the q-axis current. Therefore, we must create a reference q-axis current to maintain the speed. Then we can control the q-axis current through transformation of our axes. In this way we convert the single-variable speed control into control with more variables—speed, d-axis current, and q-axis current—and we use a vector formulation to compute the quantities that we need to control. Hence we call this method “vector control.”

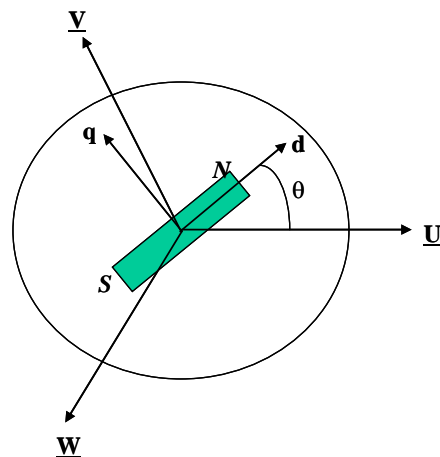


Figure 47. Stator frame to rotor frame transformation for vector control.

Now let's take a look at the detailed steps necessary for vector control. As Figure 48 shows, a profile module gives the speed command to the control algorithm at some point in time. On the right hand side, a control function outputs commands for the inverter, which is connected to the motor. This configuration has two current sensors to measure the phase U and phase W currents. The sensors are connected to the ADC on the MCU. The motor also has an encoder mounted on its rotor to give the quadrature pulses **A**, **B** and also the zero synch pulse **Z**. All three signals are sent to the input-capture and timer/counter peripheral for speed measurement.

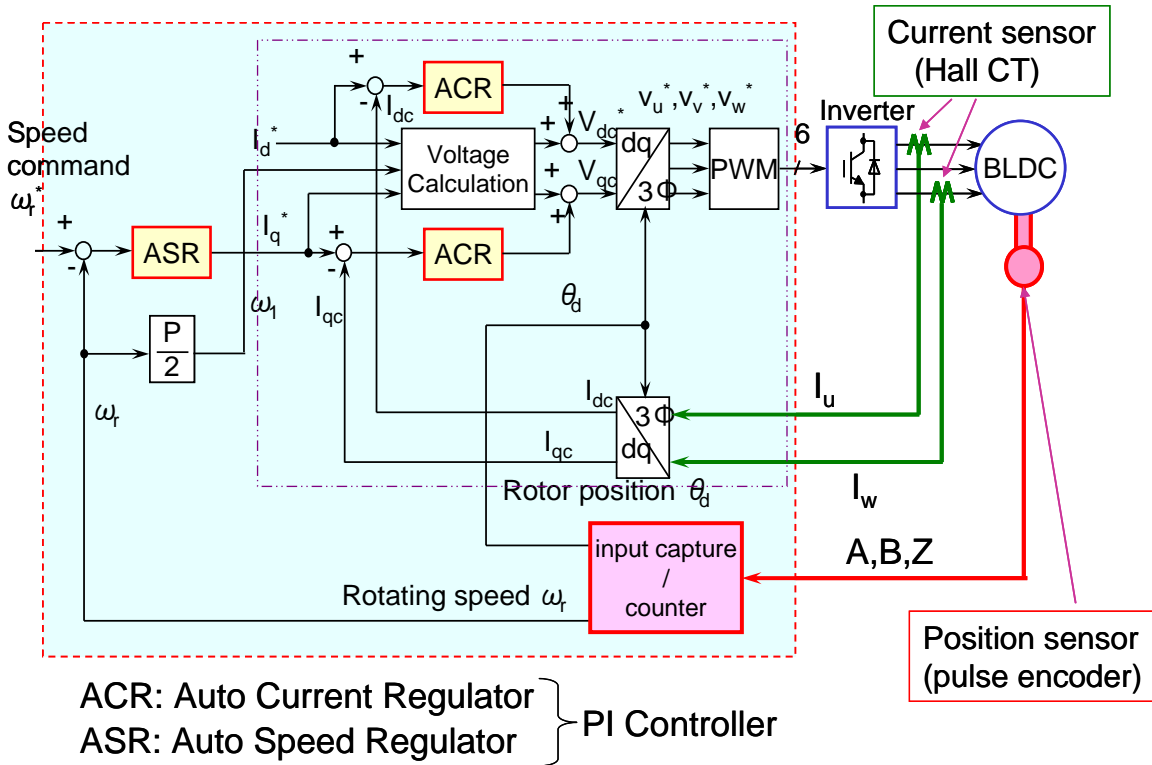


Figure 48. Vector control flow diagram.

At every carrier-frequency interrupt, three PWM signals are generated. While all three PWM signals are applied, the system measures two currents by triggering the ADC channels. During the next interrupt execution, these currents are then transformed from stator U, V, and W axes to d-q axes using matrix multiplications that involve the rotor angle q at that time. The rotor angle is measured by reading the A,B pulses and converting this reading into a proper angle. The control system's firmware is greatly helped if the MCU has a hardware timer with input capture and continuous counting of A,B pulses.

Based on the rotor position θ , stator currents are transformed in d-q axes currents as we have noted. The speed measurement is fed into the auto speed regulator (ASR), shown in Figure 48, which generates the reference q-axis current required to maintain the commanded speed. This reference q-axis current and measured q-axis currents are fed into the auto current regulator (ACR) to create q-axis voltage to be applied to the next PWM.

The reference current in the d-axis is maintained at constant level to maintain proper flux in the stator. This reference d-axis current and the measured d-axis currents are fed into a second ACR to create the d-axis voltage. Corrections are made to the voltage calculations according to the number of pole pairs and the reference currents in the d and q axes. When the final values V_d and V_q are computed, they are transformed from the rotor frame to the stator frame using inverse transformation and that rotor angle

value. Three voltages in the stator frame— V_u , V_v and V_w —are converted into the PWM values that are to be output by the three-phase timer unit.

Current measurements and auto current regulators are executed at every carrier frequency. This process, which is known as “inner loop,” uses the fastest control algorithm. In contrast, encoder measurements, and especially speed measurements, are performed at a lower rate. Therefore, the auto speed regulator and related computations are performed using a slower process called “outer loop.” A typical carrier-frequency or inner loop rate is about 4kHz or more, and the encoder-based speed computation or outer loop rate is about 500Hz or so. Occasionally the outer loop rate can drop as low as 50Hz.

Experts agree that vector control method controls the torque and flux very well, and it maintains the desired speed accurately. Vector control requires one position sensor and two current sensors to perform the necessary tasks. It also requires an MCU with high computing power so that the inner-loop and outer-loop processes can be executed properly. Additionally, the MCU must be capable of measuring two currents simultaneously, so it must have two sample-and-hold circuits in its ADC peripheral.

The vector-control method provides dynamic torque control based on exact speed measurements and current measurements. Consider an example in which the load changes during rotation. Since speed is measured several times (typically at a 500Hz rate), any load changes that affects the speed will be detected and for the next rotation, the q-axis current will be adjusted properly to maintain the same speed. If higher current is required, it will be provided. Control and system experts generally regard vector control as the reference against which the performance of other methods are compared and evaluated.

The vector-control method does have some drawbacks. It requires sensors and thus adds cost to the final implementation. Also, it mandates an MCU with high computing power, which may add cost.

In Table V1, we see a comparison of the features, accuracy, and required MCU resources for the three control methods we have covered thus far: V/f open-loop, scalar, and vector control.

Table VI. Comparison of V/f open loop, scalar and vector control.

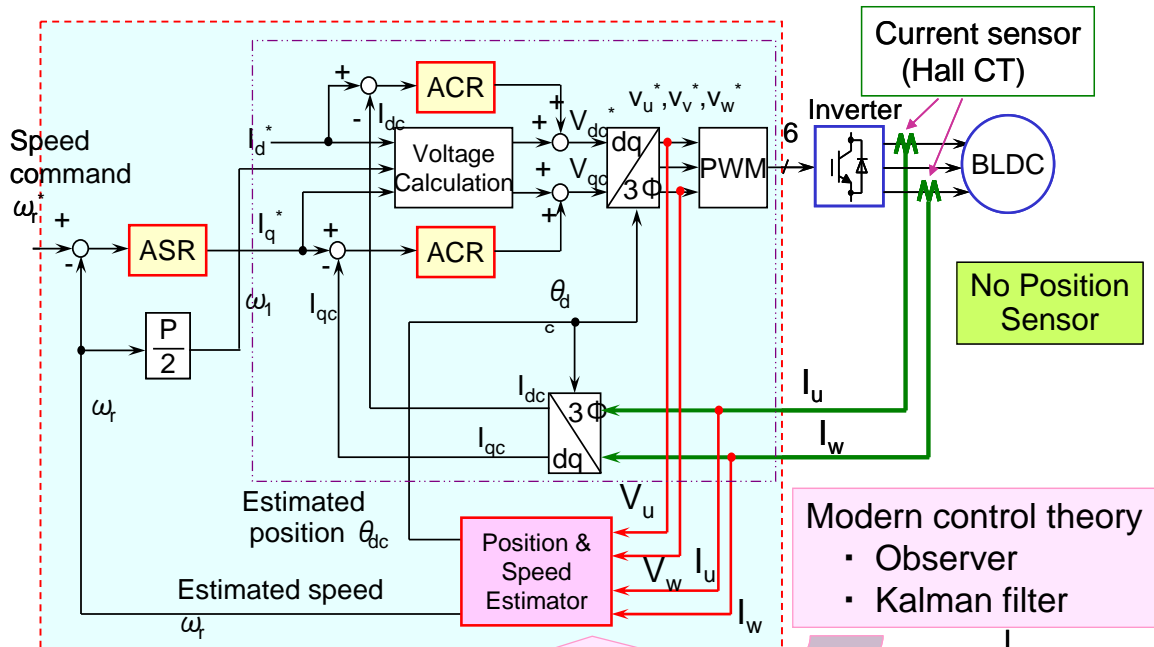
	Features	V/f open loop control	Scalar control	Vector control
1	Control method	Open loop for speed	Closed loop for speed	Closed loop for speed and current
2	Speed control accuracy	Poor	High accuracy	Very high accuracy
3	Torque control	None	Indirect only	Optimum method
4	MCU Resources	3-ph timer with dead time insertion	3-ph timer with dead time insertion	3-ph timer with dead time insertion
			Input capture w/timer to measure speed	Input capture w/timer to measure speed
				2 simultaneous channels of ADC to measure phase currents
		CPU bandwidth very reasonable	Very small increase in CPU bandwidth	Very large increase in CPU bandwidth
5	Sensors	None	Position sensor – Hall sensor, encoder, tachometer	One position sensor and two current sensors
6	Other notes	Easy to implement	Speed detection is necessary	Speed and current detection necessary
			Cost for position sensor	Cost for position and current sensors
				Cost for MCU computing power
7	Overall Score	OK	Better	Best control so far

Sensorless control

Since the vector control method we have just examined requires one position sensor and two current sensors, the final system configuration may be costly. Consumer applications, especially white goods, are very cost-sensitive and thus cannot afford this type of implementation. At the same time, these applications do not require the same performance accuracy for speed, as do industrial applications. Therefore, two other control techniques have been developed that provide adequate performance for the system, yet keep cost down. These techniques are called sensorless because they do not require any position sensors. Both methods use the same 180-degree modulation and vector control algorithm.

The first of these methods eliminates the position sensor but keeps the two current sensors. It is known as “DCCT-based sensorless vector control” and is shown in Figure 49. Because this method uses no position

sensor, angle and speed are estimated using the current measurements and voltages applied the previous PWM cycle.

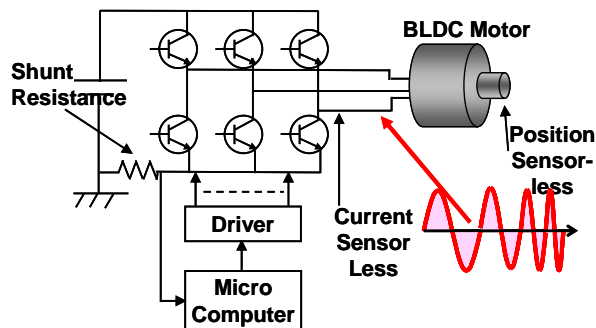


×Gain adjustment is very difficult (ASR, ACR ×2, Estimator [several parameters]) Requires Matrix Calculations

Figure 49. Position sensorless control with 2 DCCT current sensors.

The method employs a Kalman-filter approach based on principles of modern control theory, an observer-based model, and a state transition matrix. Estimated angle and speed are used together in the same vector control algorithm to control the current in the q-axis. Such an implementation requires many matrix calculations, and thus an MCU with high computing capability is a requirement. In fact, the CPU bandwidth needed is nearly double that of vector control method. Gain adjustment in the auto speed regulator and auto current regulator is very difficult. Exact motor parameters must be known, particularly the q-axis and d-axis inductance parameters, which are difficult to measure. Despite the challenges, such control is a reality and has been implemented in several applications.

6) 180-deg OSCD Sensor-less Vector Control



In a second method, the position sensor and two DCCT sensors are eliminated. Currents are measured using the shunt resistance installed on the low side of the inverter, as shown in Figure 50. This shunt resistance is a precision resistor capable of measuring the full current range of the motor. Using one shunt, we measure two currents; thus this method is known as “one shunt current detection vector control” or simply “OSCD vector control.”

Figure 50. One shunt current detection method that eliminates DCCT and position sensor.

The implementation shown in Figure 51 is similar to that of the DCCT method, but it adds one more computing block, **Current Meas**. To understand why this addition is necessary, we'll look at how the current is measured.

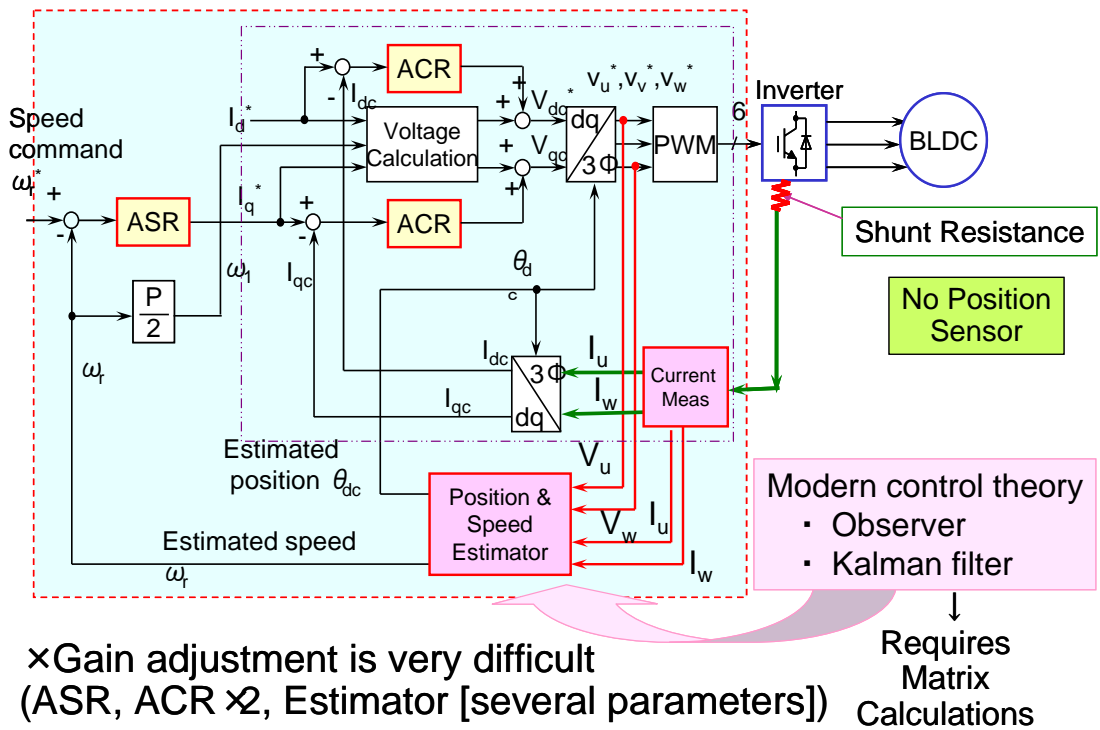


Figure 51. OSCD implementation flow with current measurement module.

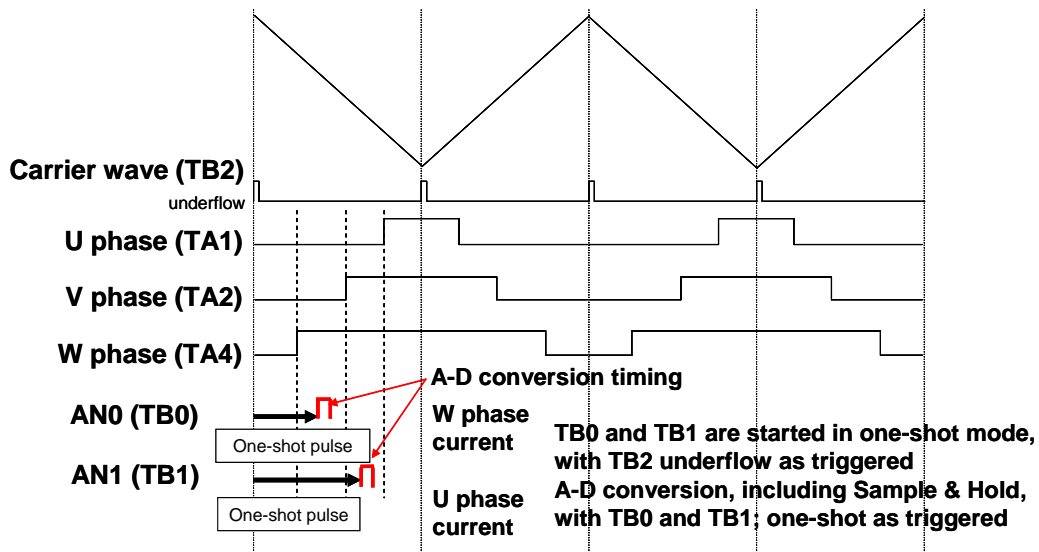


Figure 52. One shunt current measurement technique using additional timers to trigger ADC.

First, remember that our setup has only one shunt resistor. To measure individual phase currents, we must be careful. Figure 52 shows us how the three PWM outputs are applied. In this figure, the W phase has largest PWM time, V has next smaller, and U has the smallest. If we measure the shunt current between the rising edge of W and the rising edge of V, we know that only the W phase (that is, only the W_p - upper W

phase IGBT) is on at that time. So, we measure W phase current. Next, if we measure the current between the rising edge of V and the rising edge of U, then we are measuring the W and V phase current together. This also means that we are measuring the U phase current, because the sum of all currents in a star-winding motor is zero. Thus, we must make 2 current measurements at precise time during our interrupt processing. We need two other timer channels that can help us trigger the ADC at a precise time. An example is the Renesas M16C 3-phase timer unit. This unit has a link with timer channels TB0 and TB1, such that it will trigger the ADC channels AN0 and AN1 at a precise time. All we have to do is load the appropriate register values.

As part of this process, we must compare the PWM values of all three phases and determine exactly how much time we need to load channels TB0 and TB1. It is important to note that the three PWM values continue to change constantly, so that W is not the largest. Thus, we need to test the largest value every time and set the proper flags for the current we are measuring. All the comparisons, settings, and identifications required by this method make for complex processing task, one that requires significantly more code and more CPU time. The requirements for CPU bandwidth are generally more than double those of other vector-control schemes. The more complex software and higher computing power requirements keep many designers from using this method.

Performance by both sensorless methods is adequate and useful for applications that don't have tight accuracy requirements for speed. Cost is less than full vector methods and response is good—definitely better than that provided by scalar control.

All six control algorithms we have examined, from 120-degree modulation through OSCD control, have been implemented in the Renesas M16C/28 series MCU with a prototype motor control platform. Measured performance, CPU bandwidth and code size are shown in Figure 53. As we see, vector control with position and current sensors requires about 40% of the CPU bandwidth, while DCCT sensorless control requires about 74% or nearly double the bandwidth. Moreover, OSCD vector control without position and current sensors requires nearly 90% of CPU bandwidth, which is more than double the bandwidth used by vector control with sensors.

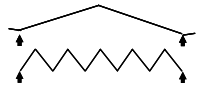
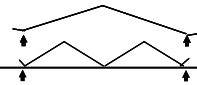
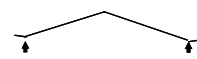
Algorithm	Carrier Freq.	ROM/RAM	Sampling Freq. (Calculating Freq.)	CPU Load Ave (Max)
120-deg Trapezoidal Wave	4KHz 20KHz	1.97KB/41B		8% (11%)
120-deg Trapezoidal Wave Sensor-less	20KHz	2.17KB/51B		30% (50%)
180-deg Sinusoidal Drive V/f	4KHz 20KHz	3.14KB/51B		12% (15%)
180-deg Vector Control – External sensor	4KHz 20KHz	4.38KB/143B		40% (42%)
180-deg (2 DCCT) Sensor-less Vector	4KHz 8KHz	6.87KB/193B		74% (75%→ 67%)
180-deg OSCD Sensor-less Vector	4KHz	10KB/1KB		88% (91%→ 91%)

Figure 53. Comparison of CPU bandwidth and code size for six speed control algorithms.

Summary

In Part 2 of this seminar, we introduced the 180-degree modulation technique and a procedure for three-phase sine-wave generation. We detailed the necessary steps for sine-wave generation, examined the code, and measured the CPU performance. We then discussed V/f open-loop control with its implementation using the M16C series device. We looked at the speed profile with three different speed settings and at a start-up ramp sequence in frequency and voltage. Next we discussed the optimization of sine-wave code and examined the CPU performance. We continued with closed-loop scalar control using a speed sensor, discussed performance of the control algorithm, and compared this method with the V/f open-loop algorithm. In the final sections, we briefly discussed vector control and the sensorless DCCT and OSCD control algorithms. We compared the CPU performance for all six algorithms, from 120-degree modulation to sensorless vector controls.

References:

- 1. Interior Permanent-Magnet Synchronous Motors for Adjustable Speed Drives**, by T. M. Jahns, G. B. Kliman and T. W. Neumann, IEEE transactions on Industry Applications, Vol. IA-22, No. 4, pp. 738-747, July/August 1986.
- 2. Dynamic Model of PM Synchronous Motors**, by Dal Y. Ohm, Drivetech Inc. Blacksburg, VA
- 3. Modeling and Parameter Characterization of Permanent Magnet Synchronous Motors**, by D. Y. Ohm, J. W. Brown and V. B. Chava, Proceedings of the 24th Annual Symposium of Incremental Motion Control Systems and Devices, San Jose, pp 81-86, June 1995.
- 4. Power Electronics and AC Drives**, by B. K. Bose, Prentice-Hall 1986.
- 5. Power Electronics and Variable Frequency Drives Technology and Applications**, Edited by Bimal K. Bose, IEEE Press, ISBN 0-7803-1084-5, 1997
- 6. Motor Control Electronics Handbook**, By Richard Valentine, McGraw-Hill, ISBN 0-07-066810-8, 1998
- 7. FIRST Course On Power Electronics and Drives**, By Ned Mohan, MNPERE, ISBN 0-9715292-2-1, 2003
- 8. Electric Drives**, By Ned Mohan, MNPERE, ISBN 0-9715292-5-6, 2003
- 9. Advanced Electric Drives, Analysis, Control and Modeling using Simulink**, By Ned Mohan, MNPERE, ISBN 0-9715292-0-5, 2001
- 10. DC Motors Speed Controls Servo Systems including Optical Encoders**, The Electro-craft Engineering Handbook by Reliance Motion Control, Inc. [No ISBN number; very old book.]
- 11. Modern Control System Theory and Application**, by Stanley M. Shinnars, Addison-Wesley, ISBN 0-201-07494-X, 1978
- 12. The Industrial Electronics Handbook**, Editor-in-Chief J. David Irwin, CRC Press and IEEE Press, ISBN 0-8493-8343-9, 1997

Appendix A Sine wave Generation Interrupt Code Example Listing.

```
#pragma INTERRUPT/B tb2_int
void tb2_int(void)
{
    static unsigned int dTheta;
#ifdef TIME_PWM
    p7_0 = 1;
#endif
    if(Update) {
        dTheta = DeltaTheta;
        Update = FALSE;
    }
    sinpt_sum = dTheta + sinpt_sum; /*Sine pointer sum .. sine skip-read value + sine
pointer sum */
    if(sinpt_sum > 23040) { /*Sine pointer sum max. value? 23040 = 360° x 64 */
        NearZero = TRUE;
        sinpt_sum = sinpt_sum - 23040; /*Sine pointer sum max value revisionsin*/
    }
    sin_pt=sinpt_sum >> 6; /* sine pointer sum / 64 */
    /*U-phase pwm command value = carrier/4 - (sinN° x (torque command value x
carrier/4))*/
    pwm_u_w = C4_DAT - (signed int)((((signed long)sin_tbl[sin_pt]*(signed
long)tq_dat)>>19);
    /*V-phase pwm command value = carrier/4 - (sinN° x (torque command value x
carrier/4))*/
    pwm_v_w = C4_DAT - (signed int)((((signed
long)sin_tbl[sin_pt+offset_v[direction]]*(signed long)tq_dat)>>19);
    /*W-phase pwm command value = carrier/4 - (sinN° x (torque command value x
carrier/4))*/
    pwm_w_w = C4_DAT - (signed int)((((signed
long)sin_tbl[sin_pt+offset_w[direction]]*(signed long)tq_dat)>>19);
    /*U-phase PWM revision*/
    if(PWM_MAX < pwm_u_w) { /*Duty at MAX?*/
        work_u = PWM_MAX; /*First half .. MAX value*/
        work_u1 = C2_DAT - PWM_MAX; /*Last half .. carrier period/2 - MAX value*/
    }
    else {
        if(PWM_MIN > pwm_u_w) { /*Duty at MIN?*/
            work_u = PWM_MIN; /*First half .. MIN value */
            work_u1 = C2_DAT - PWM_MIN; /*Last half .. carrier period/2 - MIN value*/
        }
        else { /*MIN < duty < MAX*/
            work_u = pwm_u_w; /* First half .. PWM command value*/
            work_u1 = C2_DAT-pwm_u_w; /* Last half .. carrier period/2 */
        }
        /* - U-phase PWM command value */
    }
}
/*V-phase PWM revision*/
if(PWM_MAX < pwm_v_w) { /*Duty at MAX?*/
    work_v = PWM_MAX; /*First half .. MAX value */
    work_v1 = C2_DAT-PWM_MAX; /*Last half .. carrier period/2 - MAX value*/
}
else {
    if(PWM_MIN > pwm_v_w) { /* Duty at MIN? */
```

```

        work_v = PWM_MIN;          /* First half .. MIN value */
        work_v1 = C2_DAT-PWM_MIN; /* Last half .. carrier period/2 - MIN value*/
    }
else {
        /* MIN < duty < MAX */
        work_v = pwm_v_w;          /* First half .. PWM command value */
        work_v1 = C2_DAT-pwm_v_w; /* Last half .. carrier period/2 */
        /* - V-phase PWM command value */
    }
}
/* W-phase PWM revision */
if(PWM_MAX < pwm_w_w) {          /*Duty at MAX?*/
    work_w = PWM_MAX;            /* First half .. MAX value*/
    work_w1 = C2_DAT-PWM_MAX;     /* Last half .. carrier period/2 - MAX value*/
}
else {
    if(PWM_MIN > pwm_w_w) {      /*Duty at MIN?*/
        work_w = PWM_MIN;        /*First half ..MIN */
        work_w1 = C2_DAT-PWM_MIN; /*Last half .. carrier period/2 - MIN value*/
    }
    else {
        /*MIN < duty < MAX*/
        work_w = pwm_w_w;        /*First half .. PWM command value*/
        work_w1 = C2_DAT-pwm_w_w; /*Last half .. carrier period/2 */
        /* - W-phase PWM command value*/
    }
}
ta4 = work_u;    /*Set U-phase PWM */
ta41 = work_u1;
ta1 = work_v;    /*Set V-phase PWM */
ta11 = work_v1;
ta2 = work_w;    /*Set W-phase PWM */
ta21 = work_w1;

#ifdef TIME_PWM
    p7_0 = 0;
#endif
}

```